Rakenteiden Mekaniikka (Journal of Structural Mechanics)
Vol. 52, No 2, 2019, pp. 87–113
https://rakenteidenmekaniikka.journal.fi/index
https://doi.org/10.23998/rm.75937

VERTAISARVIOITU
KOLLEGIALT GRANSKAD
PEER-REVIEWED
www.tsv.fi/tunnus

Behavior of the Abaqus CDP model in simple stress states

Alexis Fedoroff[1], Kim Calonius and Juha Kuutti

Summary. In order to use the Abaqus Concrete Damaged Plasticity (CDP) material model in simulations of reinforced concrete structures, one has to understand the effect of various parameters of the material model. Although most of the material parameters can be determined from standard concrete tests, some parameters need more advanced tests to be determined. In impact simulations one often has only limited material data available, and it makes therefore sense to study the parameter sensitivity of the material model in order to fix realistic parameter values. In this paper, the sensitivity of the simulation response with respect to two model parameters is studied: the dilation angle and the tensile to compressive meridian ratio. The sensitivity study is performed in three simple but representative stress states: the uniaxial tension state, the confined uniaxial compressive state and the pure shear state. Finally, it is discussed how these simple stress states relate to the element removal criteria, which is necessary in simulations involving fragmentation.

Key words: material modelling, elasto-plastic material with scalar damage, Abaqus Concrete Damage Plasticity

Received 22 October 2018. Accepted 8 March 2019. Published online 16 August 2019.

Introduction

About of the Abaqus CDP model

The Abaqus Concrete Damaged Plasticity (CDP) material model, as documented in the Abaqus user and theory manuals, [1], is based on two damage-plasticity theory building blocks. The first building block is a modified Drucker-Prager yield surface with Rankine tension cutoff together with a non-associative Drucker-Prager hyperbolic flow potential. The second building block is a bi-isotropic strain hardening behavior, which depends on the evolution of two scalar internal hardening variables: the compressive and tensile equivalent plastic strains. On the top of this elastic-plastic material behavior there is a possibility to couple scalar damage, i.e. stiffness degradation. The single scalar damage variable is defined to be directly dependent on the internal hardening variables. Historically, the yield surface and the non-associative flow potential that is characteristic to the CDP model was first proposed by Lubliner and his co-workers in the so called "Barcelona" model, [2]. However, the bi-isotropic hardening and the scalar stiffness degradation properties were introduced in the works of J.H. Lee and G. Fenves, [3, 4].

[1]Corresponding author. alexis.fedoroff@vtt.fi

The Abaqus CDP model can be used in its standard form, by providing in the model definition the two hardening curves and a few input parameters that control the shape of the yield surface and the flow potential. However, there is also a possibility in the CDP model to apply user defined field variable[2] dependency on any of the material parameters. For example, confined uniaxial compressive experiments show a strong dependency of the axial stress-strain curve on the hydrostatic confining pressure, [5, 6], and the Eurocode proposes a dependency of the concrete strength mean values on the confinement ratio, [7]. Likewise, there are experiments, [8], that show a dependency of the tensile axial stress and fracture energy on the loading rate. It is worthwhile to note that especially in hard missile impact simulations these field variable dependencies of compressive and tensile hardening are necessary, [9, 10].

Aims of the present publication

This paper aims to "open the black box" of the CDP model in order to investigate the behavior in depth on very simple, but representative, stress states.

Investigation of benchmark stress states

The Abaqus CDP model is calibrated in such a way that it fits the uniaxial compressive and tensile behavior of corresponding concrete tests. However, all other stress states, in particular the pure shear state, are purely a product of the CDP model. Therefore there is no guarantee that the simulation output of a shear test, for example, is a match to the corresponding physical experiment. One of the aims of this paper is, therefore, to investigate analytically or with the help of numerical computational tools the CDP model output in some very simple stress states. The benchmark stress states investigated here are the uniaxial tension, the uniaxial confined compression and the pure shear states. The choice of these three benchmark stress states is not arbitrary. Indeed, if one considers a hard missile impact on a reinforced concrete slab specimen, one can typically observe spalling and scabbing of concrete at the front and back surfaces of the slab, the formation of a punching plug in front of the missile head and finally the formation of a shear cone. With some idealization of the real life situation, the spalling and scabbing behaviors can be represented by uniaxial tensile state, the formation of the punching plug by confined uniaxial compressive state and the formation of the shear cone by the pure shear stress state.

Sensitivity analysis with respect to input parameters

Although the Abaqus CDP model is very flexible, it is not simple to use. One of the reasons is the large number of input parameters. In addition to the compressive and tensile hardening behavior input data, there is a number of parameters that determine the shape of the initial yield surface and the flow potential. In particular, the sensitivity of the model output with respect to the tensile meridian to compressive meridian ratio and the angle of dilation are under investigation. The effect of some input parameters on the yield surface shape has been studied, for example, in [11], but a proper sensitivity study of the benchmark case output with respect to input parameters is done here.

[2]The user defined field variable in Abaqus is a current material state variable that any of the CDP model built-in parameter may depend on. The dependency is implemented in the USDFLD/VUSDFLD user subroutine.

Applicability to simulations involving fragmentation

Fragmentation of concrete is the result of macroscopic crack evolution during dynamic processes up to a point where an initially connected body is split into multiple bodies, thus resulting in a change of topology. For example, the simulation of hard missile impact on concrete slab specimens by the means of finite elements is an example of fragmentation. Indeed, the formation of large scale cracks, reinforcement de-bonding and the formation of the shear cone that is pushed by the missile through the slab involves topological changes in the finite element mesh and large displacements. The simplest way to materialize these topological changes is to remove selected elements in specific locations where quasi-brittle fracture is estimated to occur. Hence the element removal criterion to be specified has two tasks: to find the correct element to remove and to find the correct conditions for removal. Various element removal criteria have been proposed, [12, 9, 10], with more or less physical intuition behind those criteria. One of the aims of this paper is to discuss the physical validity of these element removal criteria.

Table 1: Definitions of constant quantities and parameters

Denomination	Symbol		Note
Eurocode mean compressive (peak) strength	f_{cm}		(MPa)
Eurocode total strain at mean compressive (peak) strength	ϵ_{c1}		(%)
Eurocode mean tensile (peak) strength	f_{ctm}		(MPa)
Eurocode fracture energy	G_{f}		(N/m)
Eurocode secant modulus of elasticity at 0.4 f_{cm}	E_{cm}		(MPa)
dynamic increase factor for tensile stress	$\mathrm{DIF}_{\mathrm{f}}$		(-)
dynamic increase factor for fracture energy	$\mathrm{DIF}_{\mathrm{g}}$		(-)
relative tensile strain rate	SR	$=$	$\dot{\epsilon}_{\mathrm{max}}/\dot{\epsilon}^{\mathrm{QS}}_{\mathrm{max}}$
quasi static strain rate	$\dot{\epsilon}^{\mathrm{QS}}_{\mathrm{max}}$	$=$	10^{-6} 1/s
confinement ratio	CR	$=$	$\tilde{\sigma}_{\mathrm{cnf}}/f_{\mathrm{cm}}$
characteristic length	l_{ch}		(m)
equibiaxial to uniaxial initial yield ratio	$\sigma_{\mathrm{b}_0}/\sigma_{\mathrm{c}_0}$	$\in$	$[1, \infty]$
tensile to compressive meridians slope ratio	K_{c}	$=$	$q_{\mathrm{TM}}/q_{\mathrm{CM}} \in]\frac{1}{2}, 1]$
dilation angle	ϕ		
eccentricity of Drucker-Prager hyperboloid	e		
material parameter	α	$=$	$\frac{\sigma_{\mathrm{b}_0}/\sigma_{\mathrm{c}_0}-1}{2\,\sigma_{\mathrm{b}_0}/\sigma_{\mathrm{c}_0}-1} \in [0, \frac{1}{2}[$
material parameter	γ	$=$	$\frac{3(1-K_{\mathrm{c}})}{2\,K_{\mathrm{c}}-1} \in [0, \infty[$

Evaluation of the plastic increment in a general stress state

The Concrete Damaged Plasticity model is, as previously stated, an isotropically hardening non-associative[3] elastic-plastic model with optional scalar stiffness degradation. A particularity of the model is that the plastic hardening behavior can evolve independently

[3]In associative hardening the plastic flow is defined to be proportional to the gradient of the yield function. In non-associative hardening the plastic flow is arbitrary.

Table 2: Definitions of functions and variable quantities

Denomination	Symbol		Note
Heaviside function	H	:	$x \mapsto \frac{1}{2}(\mathrm{sign}(x)+1)$
Macaulay bracket	$\langle\cdot\rangle$	:	$x \mapsto \frac{1}{2}(\lvert x\rvert + x)$
total differential	$(\cdot)'$		$f'(x_0) = \frac{\mathrm{d}f}{\mathrm{d}x}\big\rvert_{x_0}$
total strain and strain rate tensor	$\boldsymbol{\epsilon}$, $\dot{\boldsymbol{\epsilon}}$		
plastic strain and strain rate tensor	$\boldsymbol{\epsilon}^{\mathrm{p}}$, $\dot{\boldsymbol{\epsilon}}^{\mathrm{p}}$		
elastic strain and strain rate tensor	$\boldsymbol{\epsilon}^{\mathrm{e}}$, $\dot{\boldsymbol{\epsilon}}^{\mathrm{e}}$		
principal plastic strain rate	$\dot{\epsilon}_i^{\mathrm{p}}$	$=$	$\boldsymbol{v}_i \cdot \dot{\boldsymbol{\epsilon}}^{\mathrm{p}} \cdot \boldsymbol{v}_i$
with corresponding unit eigenvector	$\boldsymbol{v}_i$		
maximum principal plastic strain rate	$\dot{\epsilon}^{\mathrm{p}}_{\max}$	$=$	$\max_i\{\dot{\epsilon}_i^{\mathrm{p}}\}$
minimum principal plastic strain rate	$\dot{\epsilon}^{\mathrm{p}}_{\min}$	$=$	$\min_i\{\dot{\epsilon}_i^{\mathrm{p}}\}$
equivalent plastic strain rate in compression	$\dot{\epsilon}_{\mathrm{c}}^{\mathrm{p}}$	$=$	$-(1-r)\,\dot{\epsilon}^{\mathrm{p}}_{\min}$
equivalent plastic strain rate in tension	$\dot{\epsilon}_{\mathrm{t}}^{\mathrm{p}}$	$=$	$r\,\dot{\epsilon}^{\mathrm{p}}_{\max}$
elastic stiffness fourth order tensor	$\mathbb{E}$	$=$	$\lambda\,\boldsymbol{I}\otimes\boldsymbol{I} + 2\,\mu\,\mathbb{I}$
fourth order identity tensor	$\mathbb{I}$		$\mathbb{I} : \boldsymbol{A} = \boldsymbol{A} : \mathbb{I} = \boldsymbol{A}\,,\ \forall\,\boldsymbol{A}$
second order identity tensor	$\boldsymbol{I}$		$\boldsymbol{I}\cdot\boldsymbol{A} = \boldsymbol{A}\cdot\boldsymbol{I} = \boldsymbol{A}\,,\ \forall\,\boldsymbol{A}$
Lamé first and second parameter	λ, μ		
scalar stiffness modulus, Poisson coefficient	E,ν		
scalar stiffness degradation variable	d	$\in$	$[0,1]$
damage evolution function in uniaxial compression	d_{c}	:	$\epsilon_{\mathrm{c}}^{\mathrm{p}} \mapsto d_{\mathrm{c}}(\epsilon_{\mathrm{c}}^{\mathrm{p}}) \in [0,1]$
damage evolution function in uniaxial tension	d_{t}	:	$\epsilon_{\mathrm{t}}^{\mathrm{p}} \mapsto d_{\mathrm{t}}(\epsilon_{\mathrm{t}}^{\mathrm{p}}) \in [0,1]$
effective quantity operator	$\tilde{\cdot}$	:	$x \mapsto \tilde{x} = x/(1-d)$
stress tensor	$\boldsymbol{\sigma}$	$=$	$(1-d)\,\mathbb{E} : (\boldsymbol{\epsilon} - \boldsymbol{\epsilon}^{\mathrm{p}})$
deviatoric stress	$\boldsymbol{s}$	$=$	$\boldsymbol{\sigma} - \frac{1}{3}\,\mathrm{tr}(\boldsymbol{\sigma})\,\boldsymbol{I}$
equivalent Mises stress	q	$=$	$\sqrt{3/2\,\boldsymbol{s} : \boldsymbol{s}}$
hydrostatic pressure	p	$=$	$\frac{1}{3}\,\mathrm{tr}(\boldsymbol{\sigma})$
effective stress tensor	$\tilde{\boldsymbol{\sigma}}$	$=$	$\boldsymbol{\sigma}/(1-d)$
principal stress	σ_i	$=$	$\boldsymbol{w}_i \cdot \boldsymbol{\sigma} \cdot \boldsymbol{w}_i$
with corresponding unit eigenvector	$\boldsymbol{w}_i$		
maximum principal stress	$\sigma_{\max}$	$=$	$\max_i\{\sigma_i\}$
minimum principal stress	$\sigma_{\min}$	$=$	$\min_i\{\sigma_i\}$
cohesion (yield) stress in compression	σ_{c}	:	$\epsilon_{\mathrm{c}}^{\mathrm{p}} \mapsto \sigma_{\mathrm{c}}(\epsilon_{\mathrm{c}}^{\mathrm{p}})$, $\sigma_{\mathrm{c}}(0) = \sigma_{\mathrm{c}_0}$
cohesion (yield) stress in tension	σ_{t}	:	$\epsilon_{\mathrm{t}}^{\mathrm{p}} \mapsto \sigma_{\mathrm{t}}(\epsilon_{\mathrm{t}}^{\mathrm{p}})$, $\sigma_{\mathrm{t}}(0) = \sigma_{\mathrm{t}_0}$
stress state characterization function	r	$=$	$\frac{\sum_i \langle\sigma_i\rangle}{\sum_j \lvert\sigma_j\rvert}$
average triaxiality ratio	T_{av}	$=$	$\tilde{p}/\tilde{q}$
maximum triaxiality ratio	$T_{\max}$	$=$	$\tilde{\sigma}_{\max}/\tilde{q}$
minimum triaxiality ratio	$T_{\min}$	$=$	$\tilde{\sigma}_{\min}/\tilde{q}$
triaxiality ratio tensor	$\boldsymbol{T}$	$=$	$\tilde{\boldsymbol{\sigma}}/\tilde{q}$
deviatoric triaxiality ratio tensor	$\boldsymbol{S}$	$=$	$\tilde{\boldsymbol{s}}/\tilde{q} = \boldsymbol{T} - T_{\mathrm{av}}\,\boldsymbol{I}$
effective confinement stress	$\tilde{\sigma}_{\mathrm{cnf}}$	$=$	$\langle -\tilde{p} - \tilde{q}/3\rangle$
Helmholtz free energy per volume	Ψ		
Hardening modulus in compression, tension	H_{c}, H_{t}		

"in compression" and "in tension". Therefore the hardening depends on two monotonically increasing scalar plastic flux variables. Notice also, that the entire CDP material model is based on the small strain hypothesis, which means that the additive decomposition of total strain tensor, $\boldsymbol{\epsilon} = \boldsymbol{\epsilon}^{\mathrm{e}} + \boldsymbol{\epsilon}^{\mathrm{p}}$, is valid. A more complete list of functions and variable quantities used throughout this paper can be found in Table 2. Some constant quantities and parameters are also listed in Table 1.

Characterization of the tension content in the current stress state

Uniaxial compression and tension stress states are straightforward to define. However, when the question comes to a general multiaxial stress state, it is not obvious how this state should be decomposed in a compression and tension parts. The CDP material model proposes a decomposition with the help of a dimensionless stress state characterization function, $r : \tilde{\boldsymbol{\sigma}} \mapsto r(\tilde{\boldsymbol{\sigma}}) \in [0, 1]$. Equation (1) shows the expressions of the stress state characterization function r, and its derivative $\boldsymbol{n}_r = \frac{\partial r}{\partial \tilde{\boldsymbol{\sigma}}}$.

$$r(\tilde{\boldsymbol{\sigma}}) = \frac{\sum\limits_{1\le i\le 3} \langle \sigma_i(\tilde{\boldsymbol{\sigma}}) \rangle}{\sum\limits_{1\le j\le 3} |\sigma_j(\tilde{\boldsymbol{\sigma}})|} \ , \qquad \boldsymbol{n}_r(\tilde{\boldsymbol{\sigma}}) = \frac{\sum\limits_{1\le i\le 3} \Big(\mathrm{H}\big(\sigma_i(\tilde{\boldsymbol{\sigma}})\big) - r(\boldsymbol{\sigma}) \operatorname{sign}\big(\sigma_i(\tilde{\boldsymbol{\sigma}})\big) \Big) \boldsymbol{w}_i \otimes \boldsymbol{w}_i}{\sum\limits_{1\le j\le 3} |\sigma_j(\tilde{\boldsymbol{\sigma}})|} \ . \tag{1}$$

It can be seen that everywhere in the positive quadrant $\tilde{\sigma}_1 \ge \tilde{\sigma}_2 \ge \tilde{\sigma}_3 \ge 0$ the value of the stress characterization function is $r = 1$. Likewise, everywhere in the negative quadrant $0 \ge \tilde{\sigma}_1 \ge \tilde{\sigma}_2 \ge \tilde{\sigma}_3$ the value of the stress characterization function is $r = 0$. On the deviatoric plane, when $\tilde{\sigma}_1 + \tilde{\sigma}_2 + \tilde{\sigma}_3 = 0$, the value of the stress characterization function is $r = \frac{1}{2}$.

Evolution relationships for plastic hardening

Since the plastic hardening was characterized as bi-isotropic, it is necessary now to define the corresponding two internal thermodynamic flux variables. Let's call *equivalent plastic strain in compression*[4], $\epsilon_{\mathrm{c}}^{\mathrm{p}}$ the flux variable that measures the plastic behavior "in compression". Likewise, call *equivalent plastic strain in tension*, $\epsilon_{\mathrm{t}}^{\mathrm{p}}$ the flux variable that measures the plastic behavior "in tension". The rates of these quantities are expressed in terms of the stress state characterization function, r and the plastic strain rate tensor $\dot{\boldsymbol{\epsilon}}^{\mathrm{p}}$.

$$\dot{\epsilon}_{\mathrm{c}}^{\mathrm{p}} = -(1 - r)\, \dot{\epsilon}_{\mathrm{min}}^{\mathrm{p}} = \boldsymbol{l}_{\mathrm{c}} : \dot{\boldsymbol{\epsilon}}^{\mathrm{p}} \ , \qquad\qquad \dot{\epsilon}_{\mathrm{t}}^{\mathrm{p}} = r\, \dot{\epsilon}_{\mathrm{max}}^{\mathrm{p}} = \boldsymbol{l}_{\mathrm{t}} : \dot{\boldsymbol{\epsilon}}^{\mathrm{p}} \ . \tag{2}$$

The shorthand notations $\boldsymbol{l}_{\mathrm{c}} = -(1 - r)\, \boldsymbol{v}_{\mathrm{min}} \otimes \boldsymbol{v}_{\mathrm{min}}$ and $\boldsymbol{l}_{\mathrm{t}} = r\, \boldsymbol{v}_{\mathrm{max}} \otimes \boldsymbol{v}_{\mathrm{max}}$, where $\boldsymbol{v}_{\mathrm{min}}$ is such that $\boldsymbol{v}_{\mathrm{min}} \cdot \dot{\boldsymbol{\epsilon}}^{\mathrm{p}} \cdot \boldsymbol{v}_{\mathrm{min}} = \min_i \dot{\epsilon}_i^{\mathrm{p}}$ and were $\boldsymbol{v}_{\mathrm{max}}$ is such that $\boldsymbol{v}_{\mathrm{max}} \cdot \dot{\boldsymbol{\epsilon}}^{\mathrm{p}} \cdot \boldsymbol{v}_{\mathrm{max}} = \max_i \dot{\epsilon}_i^{\mathrm{p}}$, are given for future use. The equivalent plastic strain in compression/tension variables are computed from the rate relations given in Equation (2) by time integration, $\epsilon_{\mathrm{c}}^{\mathrm{p}} = \int_0^t \dot{\epsilon}_{\mathrm{c}}^{\mathrm{p}}(\tau) \mathrm{d}\tau$ and $\epsilon_{\mathrm{t}}^{\mathrm{p}} = \int_0^t \dot{\epsilon}_{\mathrm{t}}^{\mathrm{p}}(\tau) \mathrm{d}\tau$. Notice, that since the rates of equivalent plastic strain in compression/tension are positive, it follows that the time integrals are monotonically increasing.

[4]In Abaqus, the equivalent plastic strain in compression(tension) is denoted by PEEQ(PEEQT)

Evolution relationships for stiffness degradation

Analogically to the case of plastic hardening variables, the stiffness degradation variable d depends on two damage variables. Let's call the compressive damage d_c and the tensile damage variable d_t. The stiffness degradation variable depends on the compressive and tensile damage variables as well as on the stress state characterization function r as per equation (3).

$$d(d_\mathrm{c}, d_\mathrm{t}, r) = 1 - \big(1 - s_\mathrm{t}(r)\, d_\mathrm{c}\big)\big(1 - s_\mathrm{c}(r)\, d_\mathrm{t}\big) \ , \tag{3}$$

where the functions s_t and s_c are introduced to model stiffness recovery effects associated with stress reversals. They depend on the stress state characterization function, end hence on the current effective stress state as per equation (4).

$$s_\mathrm{t}(r) = 1 - w_\mathrm{t}\, r \ , \qquad\qquad s_\mathrm{c}(r) = 1 - w_\mathrm{c}\,(1 - r) \ . \tag{4}$$

The weight factors w_t and w_c, which are assumed to be material properties, control the recovery of the tensile and compressive stiffness upon load reversal. Consider the example of a cyclic uniaxial tension and compression. In the event of a compression cycle ($r = 0$), a weight factor $w_\mathrm{c} = 1$ yields a stiffness degradation $d = d_\mathrm{c}$. In the event of a tension cycle ($r = 1$), a weight factor $w_\mathrm{t} = 1$ yields a stiffness degradation $d = d_\mathrm{t}$. A weight factor of $w_\mathrm{c} = 0$ or $w_\mathrm{t} = 0$ yields a stiffness degradation $d = 1-(1-d_\mathrm{c})(1-d_\mathrm{t})$. Considering the expressions $\dot{s}_\mathrm{t} = -w_\mathrm{t}\, \boldsymbol{n}_r : \dot{\tilde{\boldsymbol{\sigma}}}$ and $\dot{s}_\mathrm{c} = w_\mathrm{c}\, \boldsymbol{n}_r : \dot{\tilde{\boldsymbol{\sigma}}}$, one can compute the rate of the stiffness degradation variable $\dot{d}$ as follows:

$$\dot{d} = \partial_r d\, \boldsymbol{n}_r : \dot{\tilde{\boldsymbol{\sigma}}} + \partial_\mathrm{c} d\, \dot{d}_\mathrm{c} + \partial_\mathrm{t} d\, \dot{d}_\mathrm{t} \ , \tag{5}$$

where the expressions of the partial derivatives $\partial_r d$, $\partial_\mathrm{c} d$ and $\partial_\mathrm{t} d$ are given as follows:

$$\partial_r d = w_\mathrm{c} d_\mathrm{t}(1 - s_\mathrm{t} d_\mathrm{c}) - w_\mathrm{t} d_\mathrm{c}(1 - s_\mathrm{c} d_\mathrm{t}) \ , \quad \partial_\mathrm{c} d = s_\mathrm{t}(1 - s_\mathrm{c} d_\mathrm{t}) \ , \quad \partial_\mathrm{t} d = s_\mathrm{c}(1 - s_\mathrm{t} d_\mathrm{c}) \ . \tag{6}$$

Expression of the thermodynamic potential

As explained in [4], the thermodynamic potential, which in this context is the Helmholtz free energy per unit of volume, Ψ, can be expressed in terms of the Helmholtz free energy per unit of volume of undamaged material, Y, and the stiffness degradation parameter d. More specifically, we have $\Psi = (1-d)\, Y$. The expression of the Helmholtz free energy per unit of volume of undamaged material is given by $Y = Y^\mathrm{e} + Y_\mathrm{c}^\mathrm{p} + Y_\mathrm{t}^\mathrm{p}$, where the expressions for the elastic, plastic-compression and plastic-tension parts are given as follows:

$$Y^\mathrm{e} = \tfrac{1}{2}\,(\boldsymbol{\epsilon} - \boldsymbol{\epsilon}^\mathrm{p}) : \mathbb{E} : (\boldsymbol{\epsilon} - \boldsymbol{\epsilon}^\mathrm{p}) \ , \quad Y_\mathrm{c}^\mathrm{p} = \tilde{g}_\mathrm{c} - \int_0^{\epsilon_\mathrm{c}^\mathrm{p}} \tilde{\sigma}_\mathrm{c}(\epsilon)\mathrm{d}\epsilon \ , \quad Y_\mathrm{t}^\mathrm{p} = \tilde{g}_\mathrm{t} - \int_0^{\epsilon_\mathrm{t}^\mathrm{p}} \tilde{\sigma}_\mathrm{t}(\epsilon)\mathrm{d}\epsilon \ . \tag{7}$$

The compressive and tensile specific fracture energy parameters are defined as $\tilde{g}_\mathrm{c} = \int_0^\infty \tilde{\sigma}_\mathrm{c}(\epsilon)\mathrm{d}\epsilon$ and $\tilde{g}_\mathrm{t} = \int_0^\infty \tilde{\sigma}_\mathrm{t}(\epsilon)\mathrm{d}\epsilon$, respectively. Assume the Helmholtz free energy depends on thermodynamic external (observable) flux variables, $\boldsymbol{\eta} = \{\boldsymbol{\epsilon}\}$, and internal (non-observable) flux variables $\boldsymbol{\zeta} = \{\boldsymbol{\epsilon}^\mathrm{p}, d, \epsilon_\mathrm{c}^\mathrm{p}, \epsilon_\mathrm{t}^\mathrm{p}\}$. By differentiating the expression of the Helmholtz free energy per unit of volume one gets $\dot{\Psi} = (1-d)\dot{Y} - Y\dot{d}$. Simplification yields to:

$$\dot{\Psi} = (1-d)(\boldsymbol{\epsilon} - \boldsymbol{\epsilon}^\mathrm{p}) : \mathbb{E} : \big(\dot{\boldsymbol{\epsilon}} - \dot{\boldsymbol{\epsilon}}^\mathrm{p}\big) - (1-d)\tilde{\sigma}_\mathrm{c}\, \dot{\epsilon}_\mathrm{c}^\mathrm{p} - (1-d)\tilde{\sigma}_\mathrm{t}\, \dot{\epsilon}_\mathrm{t}^\mathrm{p} - Y\dot{d} \ . \tag{8}$$

One can identify from equation (8) the following expression of the stress tensor $\boldsymbol{\sigma} = (1-d)\tilde{\boldsymbol{\sigma}} = (1-d)\mathbb{E} : (\boldsymbol{\epsilon} - \boldsymbol{\epsilon}^\mathrm{p})$ as well as the expressions of the yield stresses $\sigma_\mathrm{c} = (1-d)\tilde{\sigma}_\mathrm{c}$

and $\sigma_{\mathrm{t}} = (1-d)\tilde{\sigma}_{\mathrm{t}}$. It follows that the rate of the Helmholtz free energy per unit of volume simplifies to $\dot{\Psi} = \boldsymbol{\sigma} : \dot{\boldsymbol{\epsilon}} - \boldsymbol{\sigma} : \dot{\boldsymbol{\epsilon}}^{\mathrm{p}} - Y\dot{d} - \sigma_{\mathrm{c}}\,\dot{\epsilon}^{\mathrm{p}}_{\mathrm{c}} - \sigma_{\mathrm{t}}\,\dot{\epsilon}^{\mathrm{p}}_{\mathrm{t}}$. The thermodynamic forces are therefore given by $\boldsymbol{Z} = -\partial\Psi/\partial\boldsymbol{\zeta} = \{\boldsymbol{\sigma}, Y, \sigma_{\mathrm{c}}, \sigma_{\mathrm{t}}\}$. The mechanical dissipation, $\Phi = \boldsymbol{\sigma} : \dot{\boldsymbol{\epsilon}} - \dot{\Psi}$, can, therefore be evaluated to $\Phi = \boldsymbol{Z} \cdot \dot{\boldsymbol{\zeta}}$. Since the thermodynamical forces are partial derivatives of the Helmholtz free energy, they are also functions of the thermodynamical flux variables (both external and internal), and therefore one can express the rate of the thermodynamic forces using chain derivation:

$$\dot{\boldsymbol{Z}} = \frac{\partial \boldsymbol{Z}}{\partial \boldsymbol{\eta}} \cdot \dot{\boldsymbol{\eta}} + \frac{\partial \boldsymbol{Z}}{\partial \boldsymbol{\zeta}} \cdot \dot{\boldsymbol{\zeta}} \,. \tag{9}$$

The rate of the thermodynamic force vector can be expressed as follows:

$$\begin{Bmatrix} \dot{\boldsymbol{\sigma}} \\ \dot{Y} \\ \dot{\sigma}_{\mathrm{c}} \\ \dot{\sigma}_{\mathrm{t}} \end{Bmatrix} = \begin{Bmatrix} (1-d)\mathbb{E} : (\dot{\boldsymbol{\epsilon}} - \dot{\boldsymbol{\epsilon}}^{\mathrm{p}}) - \tilde{\boldsymbol{\sigma}}\,\dot{d} \\ \tilde{\boldsymbol{\sigma}} : (\dot{\boldsymbol{\epsilon}} - \dot{\boldsymbol{\epsilon}}^{\mathrm{p}}) - \tilde{\sigma}_{\mathrm{c}}\,\dot{\epsilon}^{\mathrm{p}}_{\mathrm{c}} - \tilde{\sigma}_{\mathrm{t}}\,\dot{\epsilon}^{\mathrm{p}}_{\mathrm{t}} \\ (1-d)\tilde{\sigma}'_{\mathrm{c}}\,\dot{\epsilon}^{\mathrm{p}}_{\mathrm{c}} - \tilde{\sigma}_{\mathrm{c}}\,\dot{d} \\ (1-d)\tilde{\sigma}'_{\mathrm{t}}\,\dot{\epsilon}^{\mathrm{p}}_{\mathrm{t}} - \tilde{\sigma}_{\mathrm{t}}\,\dot{d} \end{Bmatrix} . \tag{10}$$

Therefore one can identify the partial derivatives of the thermodynamic forces:

$$\frac{\partial \boldsymbol{Z}}{\partial \boldsymbol{\zeta}} = -1 \begin{Bmatrix} (1-d)\mathbb{E} & \tilde{\boldsymbol{\sigma}} & 0 & 0 \\ \tilde{\boldsymbol{\sigma}} & 0 & \tilde{\sigma}_{\mathrm{c}} & \tilde{\sigma}_{\mathrm{t}} \\ 0 & \tilde{\sigma}_{\mathrm{c}} & -(1-d)\tilde{\sigma}'_{\mathrm{c}} & 0 \\ 0 & \tilde{\sigma}_{\mathrm{t}} & 0 & -(1-d)\tilde{\sigma}'_{\mathrm{t}} \end{Bmatrix} , \quad \frac{\partial \boldsymbol{Z}}{\partial \boldsymbol{\eta}} = \begin{Bmatrix} (1-d)\mathbb{E} \\ \tilde{\boldsymbol{\sigma}} \\ 0 \\ 0 \end{Bmatrix} . \tag{11}$$

The flow rule

The flow rule for the CDP model is expressed in the terms of a flow potential. It is assumed that the plastic strain rate, $\dot{\boldsymbol{\epsilon}}^{\mathrm{p}}$, is proportional to the gradient of a flow potential, g, with respect to the nominal stress tensor. The coefficient of proportionality $\dot{\lambda}$ is called the plastic increment. Hence, $\dot{\boldsymbol{\epsilon}}^{\mathrm{p}} = \dot{\lambda}\,\frac{\partial g}{\partial \boldsymbol{\sigma}} = \dot{\lambda}/(1-d)\,\boldsymbol{n}_g$, where the normal vector $\boldsymbol{n}_g$ is obtained from the gradient with respect to the effective stress tensor: $\boldsymbol{n}_g = \partial g/\partial\tilde{\boldsymbol{\sigma}}$. The non-associative flow rule is expressed by $\dot{\boldsymbol{\zeta}} = \dot{\lambda}\,\boldsymbol{a} + \boldsymbol{B} \cdot \dot{\boldsymbol{\eta}}$, where the vectors $\boldsymbol{a}$ and $\boldsymbol{B}$ are given the following expression:

$$\boldsymbol{a} = \frac{1}{1-d} \begin{Bmatrix} \boldsymbol{n}_g \\ (d'_{\mathrm{c}}\,\partial_{\mathrm{c}} d\,\boldsymbol{l}_{\mathrm{c}} + d'_{\mathrm{t}}\,\partial_{\mathrm{t}} d\,\boldsymbol{l}_{\mathrm{t}} - \partial_r d\,\boldsymbol{n}_r : \mathbb{E}) : \boldsymbol{n}_g \\ \boldsymbol{l}_{\mathrm{c}} : \boldsymbol{n}_g \\ \boldsymbol{l}_{\mathrm{t}} : \boldsymbol{n}_g \end{Bmatrix} , \quad \boldsymbol{B} = \begin{Bmatrix} 0 \\ \partial_r d\,\boldsymbol{n}_r : \mathbb{E} \\ 0 \\ 0 \end{Bmatrix} . \tag{12}$$

The flow potential is, in the context of the CDP model, a Drucker-Prager hyperbolic function, as shown in equation (13). It is expressed in the effective stress space.

$$g(\boldsymbol{\sigma}; d) = \sqrt{\left(e\,\tilde{\sigma}_{\mathrm{t}_0}\,\tan\phi\right)^2 + \tilde{q}^2} + \tan\phi\;\tilde{p} \,. \tag{13}$$

The expression of the normal vector, which is the gradient with respect to the effective stress tensor, is the following:

$$\boldsymbol{n}_g = \frac{\frac{3}{2}\,\tilde{\boldsymbol{s}}}{\tilde{q}\,\sqrt{1 + \left(e\,\tan\phi\,\tilde{\sigma}_{\mathrm{t}_0}/\tilde{q}\right)^2}} + \tfrac{1}{3}\,\tan\phi\,\boldsymbol{I} \,, \tag{14}$$

If one introduces the shorthand notation $c(\phi) = \tan\phi \sqrt{1 + \left(e \, \tan\phi \, \tilde{\sigma}_{t_0}/\tilde{q}\right)^2}$ and the deviatoric triaxiality ratio tensor, $\boldsymbol{S} = \tilde{\boldsymbol{s}}/\tilde{q}$, one can rewrite Equation (14) as follows:

$$\boldsymbol{n}_g = \frac{\tan\phi}{c(\phi)} \left(\tfrac{3}{2} \, \boldsymbol{S} + \tfrac{1}{3} \, c(\phi) \, \boldsymbol{I} \right) , \tag{15}$$

Expression of the yield potential

The yield potential, f, a Drucker-Prager cone with Rankine tension cutoff, is given in the effective stress space as per equation (16).

$$f(\boldsymbol{\sigma}, \sigma_c, \sigma_t; d) = \tfrac{1}{1-\alpha}\big(\tilde{q} + 3\alpha \, \tilde{p} + \beta(\tilde{\sigma}_c, \tilde{\sigma}_t) \, \langle \tilde{\sigma}_{\max} \rangle - \gamma \langle -\tilde{\sigma}_{\max} \rangle\big) - \tilde{\sigma}_c \ , \tag{16}$$

The coefficient β, which determines the sharpness of the Rankine tension cutoff is defined by the following expression: $\beta(\tilde{\sigma}_c, \tilde{\sigma}_t) = (1-\alpha)\tilde{\sigma}_c/\tilde{\sigma}_t - (1+\alpha)$. Define the normal vector as the gradient of the yield potential with respect to the effective stress tensor: $\boldsymbol{n}_f = \partial f/\partial \tilde{\boldsymbol{\sigma}}$. Also define the two scalar quantities $n_c = \partial f/\partial \tilde{\sigma}_c$ and $n_t = \partial f/\partial \tilde{\sigma}_t$. The expressions are given in equations (17a), (17b) and (17c).

$$\boldsymbol{n}_f = \frac{1}{1-\alpha} \left(\frac{\frac{3}{2} \, \tilde{\boldsymbol{s}}}{\tilde{q}} + \alpha \, \boldsymbol{I} + \Big(\beta(\tilde{\sigma}_c, \tilde{\sigma}_t) \mathrm{H}(\tilde{\sigma}_{\max}) + \gamma \, \mathrm{H}(-\tilde{\sigma}_{\max}) \Big) \, \boldsymbol{w}_{\max} \otimes \boldsymbol{w}_{\max} \right) \ , \tag{17a}$$

$$n_c = -1 + \frac{\langle \tilde{\sigma}_{\max} \rangle}{\tilde{\sigma}_t} \ , \tag{17b}$$

$$n_t = -\frac{\tilde{\sigma}_c}{\tilde{\sigma}_t} \frac{\langle \tilde{\sigma}_{\max} \rangle}{\tilde{\sigma}_t} \ . \tag{17c}$$

Equation (17a) can be simplified if one considers the deviatoric triaxiality ratio tensor and introduce the shorthand notation $3\,\chi = \beta(\tilde{\sigma}_c, \tilde{\sigma}_t)\mathrm{H}(\tilde{\sigma}_{\max}) + \gamma \, \mathrm{H}(-\tilde{\sigma}_{\max})$, as well. Hence Equation (17a) becomes:

$$\boldsymbol{n}_f = \frac{1}{1-\alpha} \left(\tfrac{3}{2} \, \boldsymbol{S} + \alpha \, \boldsymbol{I} + 3 \, \chi \, \boldsymbol{w}_{\max} \otimes \boldsymbol{w}_{\max} \right) . \tag{18}$$

Using the expressions and notations given above, one can summarize the expression of the partial derivatives of the yield function with respect to the generalized thermodynamic force and flux variables as follows:

$$\frac{\partial f}{\partial \boldsymbol{Z}} = \frac{1}{1-d} \begin{Bmatrix} \boldsymbol{n}_f \\ 0 \\ n_c \\ n_t \end{Bmatrix} , \qquad \frac{\partial f}{\partial \boldsymbol{\eta}} = \begin{Bmatrix} 0 \\ 0 \\ 0 \\ 0 \end{Bmatrix} , \qquad \frac{\partial f}{\partial \boldsymbol{\zeta}} = \frac{1}{1-d} \begin{Bmatrix} 0 \\ f(\boldsymbol{\sigma}, \sigma_c, \sigma_t; d) \\ 0 \\ 0 \end{Bmatrix} . \tag{19}$$

Expression of the plastic increment

A non-associative flow rule $\dot{\boldsymbol{\zeta}} = \dot{\lambda} \, \boldsymbol{a} + \boldsymbol{B} \cdot \dot{\boldsymbol{\eta}}$ is assumed. The plastic flow coefficient $\dot{\lambda}$ is determined from the consistency condition with respect to the yield potential f. Assume, in full generality, that the yield potential is a function of thermodynamic forces, internal thermodynamic fluxes and external thermodynamic fluxes. Then the consistency condition is expressed by

$$\frac{\partial f}{\partial \boldsymbol{Z}} \cdot \dot{\boldsymbol{Z}} + \frac{\partial f}{\partial \boldsymbol{\eta}} \cdot \dot{\boldsymbol{\eta}} + \frac{\partial f}{\partial \boldsymbol{\zeta}} \cdot \dot{\boldsymbol{\zeta}} = 0 \ . \tag{20}$$

The plastic flow coefficient can, therefore, be extracted from the consistency condition as follows:

$$\dot{\lambda} = \frac{-\left(\dfrac{\partial f}{\partial \boldsymbol{\eta}} + \dfrac{\partial f}{\partial \boldsymbol{Z}} \cdot \dfrac{\partial \boldsymbol{Z}}{\partial \boldsymbol{\eta}} + \left(\dfrac{\partial f}{\partial \boldsymbol{\zeta}} + \dfrac{\partial f}{\partial \boldsymbol{Z}} \cdot \dfrac{\partial \boldsymbol{Z}}{\partial \boldsymbol{\zeta}}\right) \cdot \boldsymbol{B}\right) \cdot \dot{\boldsymbol{\eta}}}{\left(\dfrac{\partial f}{\partial \boldsymbol{\zeta}} + \dfrac{\partial f}{\partial \boldsymbol{Z}} \cdot \dfrac{\partial \boldsymbol{Z}}{\partial \boldsymbol{\zeta}}\right) \cdot \boldsymbol{a}} \ . \tag{21}$$

Let's compute some intermediate results. First, consider the following matrix product:

$$\frac{\partial f}{\partial \boldsymbol{Z}} \frac{\partial \boldsymbol{Z}}{\partial \boldsymbol{\zeta}} = \begin{Bmatrix} -\boldsymbol{n}_f : \mathbb{E} \\ -\big(\boldsymbol{n}_f : \tilde{\boldsymbol{\sigma}} + \tilde{\sigma}_{\mathrm{c}} n_{\mathrm{c}} + \tilde{\sigma}_{\mathrm{t}} n_{\mathrm{t}}\big)/(1-d) \\ \tilde{\sigma}'_{\mathrm{c}} n_{\mathrm{c}} \\ \tilde{\sigma}'_{\mathrm{t}} n_{\mathrm{t}} \end{Bmatrix} \ . \tag{22}$$

Note first that $\tilde{\sigma}_{\mathrm{c}} n_{\mathrm{c}} + \tilde{\sigma}_{\mathrm{t}} n_{\mathrm{t}} = -\tilde{\sigma}_{\mathrm{c}}$. Then, consider the identity $\boldsymbol{n}_f : \tilde{\boldsymbol{\sigma}} - \tilde{\sigma}_{\mathrm{c}} = f(\boldsymbol{\sigma}, \sigma_{\mathrm{c}}, \sigma_{\mathrm{t}}; d)$. One gets the following expressions that are useful in the computation of the plastic increment:

$$\frac{\partial f}{\partial \boldsymbol{\zeta}} + \frac{\partial f}{\partial \boldsymbol{Z}} \cdot \frac{\partial \boldsymbol{Z}}{\partial \boldsymbol{\zeta}} = -\begin{Bmatrix} \boldsymbol{n}_f : \mathbb{E} \\ 0 \\ -\tilde{\sigma}'_{\mathrm{c}}\, n_{\mathrm{c}} \\ -\tilde{\sigma}'_{\mathrm{t}}\, n_{\mathrm{t}} \end{Bmatrix} \ , \qquad \frac{\partial f}{\partial \boldsymbol{\eta}} + \frac{\partial f}{\partial \boldsymbol{Z}} \cdot \frac{\partial \boldsymbol{Z}}{\partial \boldsymbol{\eta}} = \boldsymbol{n}_f : \mathbb{E} \ . \tag{23}$$

This leads to a rather simple form for the plastic flow coefficient:

$$\dot{\lambda} = (1-d) \frac{\boldsymbol{n}_f : \mathbb{E} : \dot{\boldsymbol{\epsilon}}}{\boldsymbol{n}_f : \mathbb{E} : \boldsymbol{n}_g + H_{\mathrm{c}} + H_{\mathrm{t}}} \ , \tag{24}$$

where the hardening modulus in compression is $H_{\mathrm{c}} = -\tilde{\sigma}'_{\mathrm{c}}\, n_{\mathrm{c}}\, \boldsymbol{l}_{\mathrm{c}} : \boldsymbol{n}_g$ and the hardening modulus in tension is $H_{\mathrm{t}} = -\tilde{\sigma}'_{\mathrm{t}}\, n_{\mathrm{t}}\, \boldsymbol{l}_{\mathrm{t}} : \boldsymbol{n}_g$. Let's simplify further the expression of the plastic coefficient. Some intermediary expressions will be provided for that purpose. In order to compute the expression $\boldsymbol{n}_f : \mathbb{E} : \boldsymbol{n}_g$ one needs the expressions of $\boldsymbol{n}_f : \boldsymbol{n}_g$, $\mathrm{tr}(\boldsymbol{n}_f)$ and $\mathrm{tr}(\boldsymbol{n}_g)$. In order to compute the expressions of the hardening moduli, one needs the expressions of $\boldsymbol{l}_{\mathrm{c}} : \boldsymbol{n}_g$ and $\boldsymbol{l}_{\mathrm{t}} : \boldsymbol{n}_g$. One gets immediately $\mathrm{tr}(\boldsymbol{n}_f) = 3(\alpha+\chi)/(1-\alpha)$ and $\mathrm{tr}(\boldsymbol{n}_g) = \tan\phi$. Also consider $\boldsymbol{w}_{\max} \otimes \boldsymbol{w}_{\max} : \boldsymbol{I} = 1$, and the identities $\boldsymbol{w}_{\max} \otimes \boldsymbol{w}_{\max} : \boldsymbol{S} = T_{\max} - T_{\mathrm{av}}$ and $\boldsymbol{w}_{\min} \otimes \boldsymbol{w}_{\min} : \boldsymbol{S} = T_{\min} - T_{\mathrm{av}}$ as well as the fact that the unit eigenvector corresponding to the i-th principal strain rate, $\boldsymbol{v}_i$ is equal to the unit eigenvector corresponding to the i-th principal stress, whenever the eigenvalues are sorted in descending order. Therefore one can consider the following expressions:

$$\boldsymbol{n}_f : \boldsymbol{n}_g = \frac{1}{1-\alpha}\left(\frac{3}{2}\left(1 + 3\chi\left(T_{\max} - T_{\mathrm{av}}\right)\right) + (\alpha+\chi)\, c(\phi)\right)\frac{\tan\phi}{c(\phi)} \ , \tag{25a}$$

$$\boldsymbol{l}_{\mathrm{c}} : \boldsymbol{n}_g = -(1-r)\left(\frac{3}{2}\left(T_{\min} - T_{\mathrm{av}}\right) + \frac{1}{3}\, c(\phi)\right)\frac{\tan\phi}{c(\phi)} \ , \tag{25b}$$

$$\boldsymbol{l}_{\mathrm{t}} : \boldsymbol{n}_g = r\left(\frac{3}{2}\left(T_{\max} - T_{\mathrm{av}}\right) + \frac{1}{3}\, c(\phi)\right)\frac{\tan\phi}{c(\phi)} \ . \tag{25c}$$

Now we shall prove that in case of active yield the ordered unit eigenvectors to the plastic strain rate tensor, $\boldsymbol{v}_i$, are actually equal to the corresponding ordered unit eigenvectors to the effective stress tensor, $\boldsymbol{w}_i$. The principal plastic strain rates can be computed from the flow rule $\dot{\boldsymbol{\epsilon}}^{\mathrm{p}} = \dot{\lambda}/(1-d)\, \boldsymbol{n}_g$ that is being substituted in the characteristic equation

$|\dot{\boldsymbol{\epsilon}}^{\mathrm{p}} - \dot{\epsilon}_i^{\mathrm{p}}\, \boldsymbol{I}| = 0$. Further substitution of the expression of $\boldsymbol{n}_g$ from Equation (15) into the characteristic equation and carrying out appropriate factorizations leads to:

$$\left(\frac{3}{2}\,\frac{\dot{\lambda}\,\tan\phi}{(1-d)\,c(\phi)\,\tilde{q}}\right)^3 \left|\tilde{\boldsymbol{\sigma}} - \left(\tilde{p} + \frac{2}{3}\,\tilde{q}\left(\frac{(1-d)\,c(\phi)}{\dot{\lambda}\,\tan\phi}\dot{\epsilon}_i^{\mathrm{p}} - \frac{1}{3}\,c(\phi)\right)\right)\boldsymbol{I}\right| = 0\ . \tag{26}$$

Since the plastic increment is non-nil in active yield state, one can infer the following expression for the principal effective stresses:

$$\tilde{\sigma}_i = \tilde{p} + \frac{2}{3}\,\tilde{q}\left(\frac{(1-d)\,c(\phi)}{\dot{\lambda}\,\tan\phi}\dot{\epsilon}_i^{\mathrm{p}} - \frac{1}{3}\,c(\phi)\right)\ , \tag{27}$$

which leads to the expression of the principal plastic strains rates in terms of the principal effective stresses:

$$\dot{\epsilon}_i^{\mathrm{p}} = \frac{\dot{\lambda}\,\tan\phi}{(1-d)\,c(\phi)}\left(\frac{3}{2}\,\frac{\tilde{\sigma}_i - \tilde{p}}{\tilde{q}} + \frac{1}{3}\,c(\phi)\right)\ . \tag{28}$$

Then we have the identity $\dot{\boldsymbol{\epsilon}}^{\mathrm{p}} \cdot \boldsymbol{v}_i = \dot{\epsilon}_i^{\mathrm{p}}\, \boldsymbol{v}_i$, which implies that $\dot{\lambda}/(1-d)\,\boldsymbol{n}_g \cdot \boldsymbol{v}_i = \dot{\epsilon}_i^{\mathrm{p}}\, \boldsymbol{v}_i$. Substituting Equation (14) in Equation (28) leads, after simplification, to $\tilde{\boldsymbol{\sigma}} \cdot \boldsymbol{v}_i = \tilde{\sigma}_i\, \boldsymbol{v}_i$. On the other hand we defined $\boldsymbol{w}_i$ as the unit eigenvector to the effective stress tensor corresponding to the i-th effective principal stress, i.e. by definition $\tilde{\boldsymbol{\sigma}} \cdot \boldsymbol{w}_i = \tilde{\sigma}_i\, \boldsymbol{w}_i$. Therefore it can be inferred that $\boldsymbol{v}_i = \boldsymbol{w}_i$. Now, let's use the information provided above to simplify the expression of the plastic increment as given in Equation (24). Consider $\boldsymbol{n}_f : \mathbb{E} : \boldsymbol{n}_g = \lambda\,\mathrm{tr}(\boldsymbol{n}_f)\mathrm{tr}(\boldsymbol{n}_g) + 2\mu\,\boldsymbol{n}_f : \boldsymbol{n}_g$, which is one of the terms in the denominator of the plastic coefficient as well as the hardening moduli H_{c} and H_{t}. Using Equations (25a), (25b) and (25c), one gets:

$$\boldsymbol{n}_f : \mathbb{E} : \boldsymbol{n}_g = \frac{3}{1-\alpha}\left(\mu\left(1 + 3\chi\left(T_{\max} - T_{\mathrm{av}}\right)\right) + \frac{3\lambda + 2\mu}{3}\,(\alpha + \chi)c(\phi)\right)\frac{\tan\phi}{c(\phi)}\ , \tag{29a}$$

$$H_{\mathrm{c}} = (1-r)\tilde{\sigma}_{\mathrm{c}}'\,n_{\mathrm{c}}\left(\frac{3}{2}\left(T_{\min} - T_{\mathrm{av}}\right) + \frac{1}{3}\,c(\phi)\right)\frac{\tan\phi}{c(\phi)}\ , \tag{29b}$$

$$H_{\mathrm{t}} = -r\tilde{\sigma}_{\mathrm{t}}'\,n_{\mathrm{t}}\left(\frac{3}{2}\left(T_{\max} - T_{\mathrm{av}}\right) + \frac{1}{3}\,c(\phi)\right)\frac{\tan\phi}{c(\phi)}\ . \tag{29c}$$

Denote $G\,k_{\mathrm{c}} = (1-r)\tilde{\sigma}_{\mathrm{c}}'\,n_{\mathrm{c}}$ and $G\,k_{\mathrm{t}} = -r\tilde{\sigma}_{\mathrm{t}}'\,n_{\mathrm{t}}$ and consider the bulk modulus, $K = \frac{3\lambda+2\mu}{3}$, and the shear modulus $G = \mu$. Denote the ratio of the bulk modulus to the shear modulus by $k = K/G$. These considerations, together with the shorthand notations $\Delta T_{\max} = T_{\max} - T_{\mathrm{av}}$ and $\Delta T_{\min} = T_{\min} - T_{\mathrm{av}}$, lead to the following rewriting of equations (29a), (29b) and (29c):

$$\boldsymbol{n}_f : \mathbb{E} : \boldsymbol{n}_g = \frac{3\,G}{1-\alpha}\Big(1 + 3\chi\,\Delta T_{\max} + k\,(\alpha + \chi)c(\phi)\Big)\frac{\tan\phi}{c(\phi)}\ , \tag{30a}$$

$$H_{\mathrm{c}} = \frac{3\,G}{1-\alpha}\Big(\frac{1-\alpha}{2}\,k_{\mathrm{c}}\,\Delta T_{\min} + \frac{1-\alpha}{9}\,k_{\mathrm{c}}\,c(\phi)\Big)\frac{\tan\phi}{c(\phi)}\ , \tag{30b}$$

$$H_{\mathrm{t}} = \frac{3\,G}{1-\alpha}\Big(\frac{1-\alpha}{2}\,k_{\mathrm{t}}\,\Delta T_{\max} + \frac{1-\alpha}{9}\,k_{\mathrm{t}}\,c(\phi)\Big)\frac{\tan\phi}{c(\phi)}\ . \tag{30c}$$

Hence, the denominator $\boldsymbol{n}_f : \mathbb{E} : \boldsymbol{n}_g + H_{\mathrm{c}} + H_{\mathrm{t}}$ in the expression of the plastic increment can be written as follows:

$$\boldsymbol{n}_f : \mathbb{E} : \boldsymbol{n}_g + H_{\mathrm{c}} + H_{\mathrm{t}} = \frac{3G\,\tan\phi}{(1-\alpha)\,c(\phi)}\,(\,A + B\,c(\phi)\,)\ , \tag{31}$$

the expressions of A and B are given as follows:

$$A = 1 + 3\chi\Delta T_{\max} + \tfrac{1}{2}(1-\alpha)(k_{\mathrm{c}}\Delta T_{\min} + k_{\mathrm{t}}\Delta T_{\max}) \ , \tag{32a}$$

$$B = (\alpha+\chi)k + \tfrac{1}{9}(1-\alpha)(k_{\mathrm{c}} + k_{\mathrm{t}}) \ . \tag{32b}$$

The numerator $\boldsymbol{n}_f : \mathbb{E} : \dot{\boldsymbol{\epsilon}}$ in the expression of the plastic increment can be computed using the following intermediary result:

$$\boldsymbol{n}_f : \dot{\boldsymbol{\epsilon}} = \frac{1}{1-\alpha}\left(\frac{3}{2}\frac{\tilde{\boldsymbol{\sigma}} : \dot{\boldsymbol{\epsilon}} - \tilde{p}\,\mathrm{tr}(\dot{\boldsymbol{\epsilon}})}{\tilde{q}} + \alpha\,\mathrm{tr}(\dot{\boldsymbol{\epsilon}}) + 3\,\chi\,\boldsymbol{w}_{\max}\cdot\dot{\boldsymbol{\epsilon}}\cdot\boldsymbol{w}_{\max}\right) \ . \tag{33}$$

Considering the triaxiality ratio notations $T_{\mathrm{av}} = \tilde{p}/\tilde{q}$ and $\boldsymbol{T} = \tilde{\boldsymbol{\sigma}}/\tilde{q}$ one can simplify the previous expression as follows:

$$\boldsymbol{n}_f : \dot{\boldsymbol{\epsilon}} = \frac{3}{1-\alpha}\left(\tfrac{1}{2}\,\boldsymbol{T} : \dot{\boldsymbol{\epsilon}} + (\tfrac{1}{3}\alpha - \tfrac{1}{2}\,T_{\mathrm{av}})\,\mathrm{tr}(\dot{\boldsymbol{\epsilon}}) + \chi\,\boldsymbol{w}_{\max}\cdot\dot{\boldsymbol{\epsilon}}\cdot\boldsymbol{w}_{\max}\right) \ . \tag{34}$$

Recalling the expression $\mathrm{tr}(\boldsymbol{n}_f) = 3(\alpha+\chi)/(1-\alpha)$, $\lambda = G(k-\frac{2}{3})$, $\mu = G$ and $k = K/G$ and since we have the following expression: $\boldsymbol{n}_f : \mathbb{E} : \dot{\boldsymbol{\epsilon}} = \lambda\,\mathrm{tr}(\boldsymbol{n}_f)\,\mathrm{tr}(\dot{\boldsymbol{\epsilon}}) + 2\mu\,\boldsymbol{n}_f : \dot{\boldsymbol{\epsilon}}$, one can simplify the numerator of the plastic increment as follows:

$$\boldsymbol{n}_f : \mathbb{E} : \dot{\boldsymbol{\epsilon}} = \frac{3G}{1-\alpha}\left(\boldsymbol{T} + \left(\tfrac{2}{3}\alpha - T_{\mathrm{av}} + (k-\tfrac{2}{3})(\alpha+\chi)\right)\boldsymbol{I} + 2\chi\,\boldsymbol{w}_{\max}\otimes\boldsymbol{w}_{\max}\right) : \dot{\boldsymbol{\epsilon}} \ . \tag{35}$$

Substituting Equations (31) and (35) into the expression of the plastic increment as given by Equation (24) gives:

$$\dot{\lambda} = (1-d)\frac{\left(\boldsymbol{T} + \left((\alpha+\chi)k - T_{\mathrm{av}} - \tfrac{2}{3}\chi\right)\boldsymbol{I} + 2\chi\,\boldsymbol{w}_{\max}\otimes\boldsymbol{w}_{\max}\right) : \dot{\boldsymbol{\epsilon}}}{A + B\,c(\phi)}\,\frac{c(\phi)}{\tan\phi} \ . \tag{36}$$

Hence the expression of the plastic increment can be given as $\frac{\dot{\lambda}}{1-d}\frac{\tan\phi}{c(\phi)} = \boldsymbol{\Omega} : \dot{\boldsymbol{\epsilon}}$, where the matrix $\boldsymbol{\Omega}$ can be expressed as follows:

$$\boldsymbol{\Omega} = \frac{\boldsymbol{T} + \left((\alpha+\chi)k - T_{\mathrm{av}} - \tfrac{2}{3}\chi\right)\boldsymbol{I} + 2\chi\,\boldsymbol{w}_{\max}\otimes\boldsymbol{w}_{\max}}{1 + 3\chi\Delta T_{\max} + \frac{1-\alpha}{2}(k_{\mathrm{c}}\Delta T_{\min} + k_{\mathrm{t}}\Delta T_{\max}) + \left((\alpha+\chi)k + \frac{1-\alpha}{9}(k_{\mathrm{c}}+k_{\mathrm{t}})\right)c(\phi)} \tag{37}$$

Application to the uniaxial tensile stress state

Consider a uniaxial tensile state, where the stress tensor is given by $\tilde{\boldsymbol{\sigma}} = \mathrm{diag}(\tilde{\sigma}_{\mathrm{axi}}, 0, 0)$, where $\tilde{\sigma}_{\mathrm{axi}}$ is considered a positive value. The strain state is therefore diagonal, $\boldsymbol{\epsilon} = \mathrm{diag}(\epsilon_1, \epsilon_2, \epsilon_3)$, with $\epsilon_1 \geq \epsilon_2 = \epsilon_3$, and it is assumed that the material state is driven by the axial strain ϵ_1. Substituting the stress state in the yield potential expression, (16), one gets $\tilde{\sigma}_{\mathrm{axi}} \leq \tilde{\sigma}_{\mathrm{t}}$ as the yield condition in uniaxial tensile stress state. Other parameter values are summarized in Table 3.

Expressions of the plastic strain rate and effective stress rate

Substitution of the values exposed in Table 3 in Equation (37) gives the expression of the plastic increment:

$$\boldsymbol{\Omega} : \dot{\boldsymbol{\epsilon}} = \frac{E\,\dot{\epsilon}_1}{\left(E + \tilde{\sigma}'_{\mathrm{t}}\right)\left(1 + \frac{1}{3}c(\phi)\right)} \ . \tag{38}$$

Table 3: Parameter values in uniaxial tensile stress state

Symbol		Value	Symbol		Value	Symbol		Value
$\tilde{p}$	=	$\frac{1}{3}\tilde{\sigma}_{\text{axi}}$	$\Delta T_{\max}$	=	$\frac{2}{3}$	r	=	1
$\tilde{q}$	=	$\tilde{\sigma}_{\text{axi}}$	$\Delta T_{\min}$	=	$-\frac{1}{3}$	χ	=	$\frac{1}{3}\beta$
T_{av}	=	$\frac{1}{3}$	$\boldsymbol{T}$	=	$\text{diag}(1,0,0)$	k_{c}	=	0
$T_{\max}$	=	1	n_{c}	=	0	k_{t}	=	$\frac{\tilde{\sigma}_{\text{c}}}{\tilde{\sigma}_{\text{t}}}\,\tilde{\sigma}'_{\text{t}}/G$
$T_{\min}$	=	0	n_{t}	=	$-\frac{\tilde{\sigma}_{\text{c}}}{\tilde{\sigma}_{\text{t}}}$	$\boldsymbol{w}_{\max}$	=	$(1,0,0)$

Further substitution of equation (38) in the expressions of the plastic strain rates leads to the following expressions:

$$\dot{\epsilon}^{\text{p}}_1 = \frac{E\,\dot{\epsilon}_1}{E+\tilde{\sigma}'_{\text{t}}}\ , \qquad\qquad \dot{\epsilon}^{\text{p}}_2 + \dot{\epsilon}^{\text{p}}_3 = -\frac{E\,\dot{\epsilon}_1}{E+\tilde{\sigma}'_{\text{t}}}\,\frac{1-\frac{2}{3}\,c(\phi)}{1+\frac{1}{3}\,c(\phi)}\ . \tag{39}$$

The expression of the equivalent plastic strain rate in tension, $\dot{\epsilon}^{\text{p}}_{\text{t}} = r\,\dot{\epsilon}^{\text{p}}_1$, whilst $r = 1$ is therefore simply:

$$\dot{\epsilon}^{\text{p}}_{\text{t}} = \frac{E\,\dot{\epsilon}_1}{E+\tilde{\sigma}'_{\text{t}}}\ . \tag{40}$$

Looking at the expressions of the plastic strain rates in the non-axial directions, $\dot{\epsilon}^{\text{p}}_2+\dot{\epsilon}^{\text{p}}_3$, one can see a dependence on the dilation angle ϕ. When the dilation angle value tends to 56.3 degrees, the rate $\dot{\epsilon}^{\text{p}}_2 + \dot{\epsilon}^{\text{p}}_3$ tends to zero. Substitution of the plastic strain rate expression in the differential stress-strain relation, $\dot{\tilde{\sigma}}_{\text{axi}} = E\,(\dot{\epsilon}_1 - \dot{\epsilon}^{\text{p}}_1)$, leads to the expression of the effective axial stress rate:

$$\dot{\tilde{\sigma}}_{\text{axi}} = \frac{E\,\tilde{\sigma}'_{\text{t}}}{E+\tilde{\sigma}'_{\text{t}}}\,\dot{\epsilon}_1\ . \tag{41}$$

Stress-strain plot in monotonic loading conditions

The expression of the axial effective stress rate, as given in Equation (41), can be used in numerical integrations provided that the total axial strain rate is given. If we further assume that the loading conditions are monotonic, one can integrate analytically the stress rate and total strain rate expressions with respect to the equivalent plastic strain in tension, $\epsilon^{\text{p}}_{\text{t}}$, to obtain a parametric expression of the axial effective stress - axial total strain plot.

$$\dot{\tilde{\sigma}}_1 = \tilde{\sigma}'_{\text{t}}\,\dot{\epsilon}^{\text{p}}_{\text{t}}\ , \qquad\qquad \dot{\epsilon}_1 = (1+\tilde{\sigma}'_{\text{t}}/E)\,\dot{\epsilon}^{\text{p}}_{\text{t}}\ . \tag{42}$$

Equation (42) can be directly time-integrated. The integral is given by:

$$\tilde{\sigma}_1(\epsilon^{\text{p}}_{\text{t}}) = \tilde{\sigma}_{\text{t}}(\epsilon^{\text{p}}_{\text{t}})\ , \qquad\qquad \epsilon_1(\epsilon^{\text{p}}_{\text{t}}) = \epsilon^{\text{p}}_{\text{t}} + \tilde{\sigma}_{\text{t}}(\epsilon^{\text{p}}_{\text{t}})/E\ . \tag{43}$$

Consider now a specific hardening evolution in tension, for example a exponential one as suggested in [4]:

$$\tilde{\sigma}_{\text{t}}(\epsilon^{\text{p}}_{\text{t}}) = \tilde{\sigma}_{\text{t}_0}\exp(-b_{\text{t}}\,\epsilon^{\text{p}}_{\text{t}})\ , \tag{44}$$

where the constants $\tilde{\sigma}_{\text{t}_0}$ and b_{t} can be computed using Eurocode concrete values, [7]. Then we have $\tilde{\sigma}_{\text{t}_0}$ equal to the concrete mean tensile strength and the constant b_{t} is solved out

from the fracture energy integral. It is assumed that all these values are rate dependent. Dynamic increase factors $\mathrm{DIF_f}$ and $\mathrm{DIF_g}$ are assumed to be functions of the relative tensile strain rate, SR. One can approximate the dynamic increase factor by piecewise linear functions on the logarithmic scale, as suggested in [13, 8, 14, 15]. In these computations we have used $\mathrm{DIF_f} = 1 + \frac{1}{12}\log(\mathrm{SR})$ for $\log(\mathrm{SR}) < 6$ and $\mathrm{DIF_f} = -15 + \frac{11}{4}\log(\mathrm{SR})$ for $\log(\mathrm{SR}) \geq 6$. Likewise, we have used $\mathrm{DIF_g} = 1 + \frac{5}{6}\log(\mathrm{SR})$ for $\log(\mathrm{SR}) < 6$ and $\mathrm{DIF_g} = -60 + 11\log(\mathrm{SR})$ for $\log(\mathrm{SR}) \geq 6$. The constant $\tilde{\sigma}_{\mathrm{t}_0}$ is then given by $\tilde{\sigma}_{\mathrm{t}_0} = \mathrm{DIF_f}\, f_{\mathrm{ctm}}$. The constant b_{t} is obtained from the equation: $\mathrm{DIF_g}\, G_{\mathrm{F}} = l_{\mathrm{ch}} \int_0^\infty \tilde{\sigma}_{\max}(\epsilon_{\mathrm{t}}^{\mathrm{p}})\, \epsilon'_{\max}(\epsilon_{\mathrm{t}}^{\mathrm{p}})\, \mathrm{d}\epsilon_{\mathrm{t}}^{\mathrm{p}}$.

$$b_{\mathrm{t}} = \frac{\mathrm{DIF_f}\, f_{\mathrm{ctm}}}{\mathrm{DIF_g}\, G_{\mathrm{F}}/l_{\mathrm{ch}} + \frac{1}{2}\,(\mathrm{DIF_f}\, f_{\mathrm{ctm}})^2/E_{\mathrm{cm}}}\ . \tag{45}$$

Notice that the hardening evolution we have chosen is strain rate dependent due to the dynamic increase factor present in Equation (45). Figure 1a shows the stress-strain plots and Figure 1b the stress-displacement plots in uniaxial tensile state for C30/37 concrete.

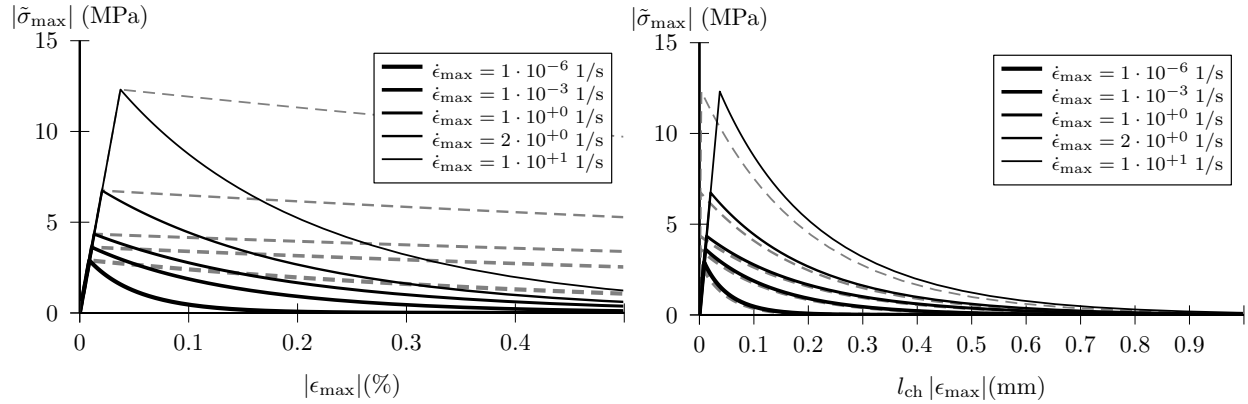

(a) Effective stress - total strain plot

(b) Effective stress - total displacement plot

Figure 1: Total axial stress evolution in uniaxial tensile state (C30/37 concrete, solid: l_{ch}=100mm, dashed: l_{ch}=10mm)

Application to the confined uniaxial compressive stress state

Consider a confined uniaxial compressive stress state, which is a superposition of a hydrostatic confinement of magnitude, $\tilde{\sigma}_{\mathrm{cnf}} \geq 0$ and an additional axial compressive stress of magnitude, $\tilde{\sigma}_{\mathrm{axi}} \geq 0$. Hence the stress tensor in such a confined uniaxial stress state is given by:

$$\tilde{\boldsymbol{\sigma}} = -\tilde{\sigma}_{\mathrm{cnf}}\, \boldsymbol{I} + \mathrm{diag}(0, 0, -\tilde{\sigma}_{\mathrm{axi}})\ , \tag{46}$$

The strain state is therefore diagonal, $\boldsymbol{\epsilon} = \mathrm{diag}(\epsilon_1, \epsilon_2, \epsilon_3)$, with $\epsilon_1 = \epsilon_2 \geq \epsilon_3$, and it is assumed that the material state is driven by the axial strain ϵ_3, and also by the hydrostatic confinement magnitude, $\tilde{\sigma}_{\mathrm{cnf}}$. One can then easily compute the deviatoric stress tensor, $\tilde{\boldsymbol{s}} = \mathrm{diag}(1, 1, -2)\, \tilde{\sigma}_{\mathrm{axi}}/3$. In a general triaxial stress state the confinement stress can be evaluated to $\tilde{\sigma}_{\mathrm{cnf}} = \langle -\tilde{p} - \tilde{q}/3 \rangle$, which matches with the definition we have given in Equation (46). Denote the confinement ratio by $T_{\mathrm{cnf}} = \tilde{\sigma}_{\mathrm{cnf}}/\tilde{\sigma}_{\mathrm{axi}}$. Other useful parameter values are summarized in Table 4.

Table 4: Parameter values in confined uniaxial compressive stress state

Symbol		Value	Symbol		Value	Symbol		Value
$\tilde{p}$	=	$-\tilde{\sigma}_{\mathrm{cnf}} - \frac{1}{3}\tilde{\sigma}_{\mathrm{axi}}$	$\Delta T_{\max}$	=	$\frac{1}{3}$	$\boldsymbol{T}$	=	$-\mathrm{diag}(T_{\mathrm{cnf}}, T_{\mathrm{cnf}}, 1+T_{\mathrm{cnf}})$
$\tilde{q}$	=	$\tilde{\sigma}_{\mathrm{axi}}$	$\Delta T_{\min}$	=	$-\frac{2}{3}$	χ	=	$\frac{1}{3}\gamma$
T_{av}	=	$-T_{\mathrm{cnf}} - \frac{1}{3}$	r	=	0	k_{c}	=	$-\tilde{\sigma}'_{\mathrm{c}}/G$
$T_{\max}$	=	$-T_{\mathrm{cnf}}$	n_{c}	=	-1	k_{t}	=	0
$T_{\min}$	=	$-T_{\mathrm{cnf}} - 1$	n_{t}	=	0	$\boldsymbol{w}_{\max}$	$\in$	$\{(1,0,0),(0,1,0)\}$

Expressions of the plastic strain rates

Substitution of the values exposed in the previous paragraph in Equation (37) gives the expression of the plastic increment:

$$\boldsymbol{\Omega} : \dot{\boldsymbol{\epsilon}} = -\frac{E\,\dot{\epsilon}_3 + \left(\frac{1+2\alpha+\gamma}{1-\alpha} - 2\nu\right)\dot{\tilde{\sigma}}_{\mathrm{cnf}}}{\left(E + \tilde{\sigma}'_{\mathrm{c}}\right)\left(1 - \frac{1}{3}c(\phi)\right)} \,. \tag{47}$$

Substitution of equation (47) in the expressions of the plastic strains leads to the following expressions:

$$\dot{\epsilon}^{\mathrm{p}}_1 + \dot{\epsilon}^{\mathrm{p}}_2 = -\dot{\epsilon}^{\mathrm{p}}_3 \frac{1 + \frac{2}{3}\,c(\phi)}{1 - \frac{1}{3}\,c(\phi)} \,, \qquad \dot{\epsilon}^{\mathrm{p}}_3 = \frac{E}{E + \tilde{\sigma}'_{\mathrm{c}}}\left(\dot{\epsilon}_3 + \left(\frac{1+2\alpha+\gamma}{1-\alpha} - 2\nu\right)\frac{\dot{\tilde{\sigma}}_{\mathrm{cnf}}}{E}\right) \,. \tag{48}$$

Recalling that $\gamma = 3(1-K_{\mathrm{c}})/(2\,K_{\mathrm{c}}-1)$, and in uniaxial confined compression stress state $\dot{\epsilon}^{\mathrm{p}}_{\mathrm{c}} = -\dot{\epsilon}^{\mathrm{p}}_3$, one can write the expression of the equivalent plastic strain rate as follows:

$$\dot{\epsilon}^{\mathrm{p}}_{\mathrm{c}} = -\frac{E}{E + \tilde{\sigma}'_{\mathrm{c}}}\left(\dot{\epsilon}_3 + \left(\frac{1+2\alpha}{1-\alpha} - 2\nu + \frac{3(1-K_{\mathrm{c}})}{(2\,K_{\mathrm{c}}-1)(1-\alpha)}\right)\frac{\dot{\tilde{\sigma}}_{\mathrm{cnf}}}{E}\right) \,. \tag{49}$$

From the expression of the equivalent plastic strain rate in compression, as shown in Equation (49), one can infer the following. If the confinement stress, $\tilde{\sigma}_{\mathrm{cnf}}$, is held constant, then the equivalent plastic strain rate in compression depends only on the total axial strain rate and the slope of the cohesion stress in compression. In case of hardening (slope is positive), $\dot{\epsilon}^{\mathrm{p}}_{\mathrm{c}} \leq \dot{\epsilon}_3$. In case of softening (slope is negative), $\dot{\epsilon}^{\mathrm{p}}_{\mathrm{c}} \geq \dot{\epsilon}_3$. If we have active confinement occurring, i.e. $\dot{\tilde{\sigma}}_{\mathrm{cnf}} > 0$, then the equivalent plastic strain rate in compression is larger than in the constant confinement case. On the other hand, if we have deconfinement, i.e. $\dot{\tilde{\sigma}}_{\mathrm{cnf}} < 0$, then the equivalent plastic strain rate in compression is smaller than in the constant confinement case. It is worth to note that if the value of the tensile to compressive meridian slope ratio, K_{c}, tends to the value of $\frac{1}{2}$, then the value of the equivalent plastic strain rate in compression tends to infinity, which is physically not admissible. Likewise, if K_{c} tends to the value 1, then the effect of the confinement stress rate on the value of the equivalent plastic strain rate in compression is minimized.

Looking at the expressions of the plastic strain rates in the confining directions, $\dot{\epsilon}^{\mathrm{p}}_1 + \dot{\epsilon}^{\mathrm{p}}_2$, one can see a strong dependence on the dilation angle ϕ. When the dilation angle value tends to 71.6 degrees, then $\dot{\epsilon}^{\mathrm{p}}_1$ and $\dot{\epsilon}^{\mathrm{p}}_2$ tends to infinity, which is physically not admissible. In order to keep the ratios $\dot{\epsilon}^{\mathrm{p}}_1/\dot{\epsilon}^{\mathrm{p}}_{\mathrm{c}}$ and $\dot{\epsilon}^{\mathrm{p}}_2/\dot{\epsilon}^{\mathrm{p}}_{\mathrm{c}}$ within the "reasonable" bound of 80 to 120 percent, the value of the dilation angle must be kept within the range of 26.6 to 43.7 degrees. Also, experience from numerical simulations of impact loaded concrete structures shows that a too large value for the dilation angle leads to complications in the explicit time integration and failure of the simulation.

Expression of the axial effective stress rate

Substitution of the plastic strain rate into the differentiated stress-strain relationship, $\dot{\tilde{\sigma}}_{\text{axi}} = -E\,(\dot{\epsilon}_3 - \dot{\epsilon}_3^{\text{p}}) - (1-2\nu)\,\dot{\tilde{\sigma}}_{\text{cnf}}$, yields the following expression of the additional axial effective stress rate:

$$\dot{\tilde{\sigma}}_{\text{axi}} = -\frac{E}{E+\tilde{\sigma}'_{\text{c}}}\left(\tilde{\sigma}'_{\text{c}}\,\dot{\epsilon}_3 + \left((1-2\,\nu)\frac{\tilde{\sigma}'_{\text{c}}}{E} - \frac{3\alpha+\gamma}{1-\alpha}\right)\dot{\tilde{\sigma}}_{\text{cnf}}\right)\,. \tag{50}$$

Considering the fact that $\dot{\tilde{\sigma}}_3 = -(\dot{\tilde{\sigma}}_{\text{axi}} + \dot{\tilde{\sigma}}_{\text{cnf}})$, one can write the expression of the total axial stress rate:

$$\dot{\tilde{\sigma}}_3 = \frac{E}{E+\tilde{\sigma}'_{\text{c}}}\left(\tilde{\sigma}'_{\text{c}}\,\dot{\epsilon}_3 - \left(2\,\nu\frac{\tilde{\sigma}'_{\text{c}}}{E} - \frac{1+2\alpha+\gamma}{1-\alpha}\right)\dot{\tilde{\sigma}}_{\text{cnf}}\right)\,. \tag{51}$$

Stress-strain plot in monotonic loading conditions

The expression of the additional axial effective stress rate, as given in Equation (51), can be used in numerical integrations provided that the total axial strain rate is given. If we further assume that the loading conditions are monotonic, one can integrate analytically the stress rate and total strain rate expressions with respect to the equivalent plastic strain in compression, $\epsilon_{\text{c}}^{\text{p}}$, to obtain a parametric expression of the axial effective stress - axial total strain plot.

$$\dot{\tilde{\sigma}}_3 = -\tilde{\sigma}'_{\text{c}}\,\dot{\epsilon}_{\text{c}}^{\text{p}} - \frac{1+2\alpha+\gamma}{1-\alpha}\,\dot{\tilde{\sigma}}_{\text{cnf}}\,, \tag{52a}$$

$$\dot{\epsilon}_3 = -\left(1+\frac{\tilde{\sigma}'_{\text{t}}}{E}\right)\dot{\epsilon}_{\text{c}}^{\text{p}} - \left(\frac{1+2\alpha+\gamma}{1-\alpha} - 2\,\nu\right)\dot{\tilde{\sigma}}_{\text{cnf}}\,. \tag{52b}$$

Equations (52a) and (52b) can be directly time-integrated. The integral is given by:

$$|\tilde{\sigma}_3(\epsilon_{\text{c}}^{\text{p}})| = \tilde{\sigma}_{\text{c}}(\epsilon_{\text{c}}^{\text{p}}) + \frac{1+2\alpha+\gamma}{1-\alpha}\,\tilde{\sigma}_{\text{cnf}}\,, \tag{53a}$$

$$|\epsilon_3(\epsilon_{\text{c}}^{\text{p}})| = \epsilon_{\text{c}}^{\text{p}} + \frac{\tilde{\sigma}_{\text{c}}(\epsilon_{\text{c}}^{\text{p}})}{E} + \left(\frac{1+2\alpha+\gamma}{1-\alpha} - 2\,\nu\right)\frac{\tilde{\sigma}_{\text{cnf}}}{E}\,. \tag{53b}$$

Consider now a specific hardening evolution in compression, for example a exponential one as suggested in [4]:

$$\tilde{\sigma}_{\text{c}}(\epsilon_{\text{c}}^{\text{p}}) = \tilde{\sigma}_{\text{c}_0}\big(\,(1+a_{\text{c}})\exp(-b_{\text{c}}\,\epsilon_{\text{c}}^{\text{p}}) - a_{\text{c}}\exp(-2\,b_{\text{c}}\,\epsilon_{\text{c}}^{\text{p}})\,\big)\,, \tag{54}$$

where the constants $\tilde{\sigma}_{\text{c}_0}$, a_{c} and b_{c} can be computed from the Eurocode concrete values, [7]. First, notice that the Eurocode assumes that the initial yield stress in uniaxial compression is 40% of the mean concrete strength value. Hence, $\tilde{\sigma}_{\text{c}_0} = 0.4\,f_{\text{cm}}$. Notice that the initial yield stress is independent of the confinement stress. The mean concrete cylinder strength at current confinement can be computed as the product of the unconfined mean concrete cylinder strength multiplied by a confinement increase factor. It is suggested in the Eurocode that the confinement increase factor on the mean concrete cylinder strength, ζ, is a piecewise linear function of the confinement ratio: $\zeta(\text{CR}) = 1.0 + 5.0\,\text{CR}$ for $\text{CR} \leq 0.05$ and $\zeta(\text{CR}) = 1.125 + 2.5\,\text{CR}$ for $\text{CR} \geq 0.05$. The confinement increase factor on the strain is equal to the confinement increase factor on the mean concrete cylinder strength to the second power, $\epsilon_{\text{c}_1}(\text{CR}) = \zeta^2(\text{CR})\,\epsilon_{\text{c}_1}$. Then, by substituting the values for

mean concrete cylinder strength and the corresponding total strain at current confinement ratio in Equations 53a and 53b, one gets the value, at current confinement ratio, of the equivalent plastic strain when the peak stress is reached:

$$\epsilon^{\mathrm{p}}_{\mathrm{c}_1}(\mathrm{CR}) = \epsilon_{\mathrm{c}_1}(\mathrm{CR}) + \big(\, 2\,\nu\,\mathrm{CR} - \zeta(\mathrm{CR})\,\big)\,\frac{\mathrm{f}_{\mathrm{cm}}}{E}\ . \tag{55}$$

For shorthand, consider the notation $\mu(\mathrm{CR}) = \tilde{\sigma}_{\mathrm{c}}\big(\,\epsilon^{\mathrm{p}}_{\mathrm{c}_1}(\mathrm{CR})\,\big)/\tilde{\sigma}_{\mathrm{c}_0}$ (not to be confused with Lamé second parameter). From (53a) it follows that $\mu(\mathrm{CR}) = 2.5\,\big(\,\zeta(\mathrm{CR}) - \frac{1+2\alpha+\gamma}{1-\alpha}\,\mathrm{CR}\,\big)$. The material parameters $a_{\mathrm{c}}(\mathrm{CR})$ and $b_{\mathrm{c}}(\mathrm{CR})$ are then given by Equations (56) and (57).

$$a_{\mathrm{c}}(\mathrm{CR}) = 2\,\mu(\mathrm{CR}) + 2\,\sqrt{\mu^2(\mathrm{CR}) - \mu(\mathrm{CR})} - 1\ , \tag{56}$$

$$b_{\mathrm{c}}(\mathrm{CR}) = -\frac{1}{\epsilon^{\mathrm{p}}_{\mathrm{c}_1}(\mathrm{CR})}\,\ln\left(\frac{1 + a_{\mathrm{c}}(\mathrm{CR})}{2\,a_{\mathrm{c}}(\mathrm{CR})}\right)\ . \tag{57}$$

Notice, that from Equation (56), one gets the constraint $\mu \geq 1$, whence one can compute the theoretical upper limit for the confinement ratio, $\mathrm{CR}^{\mathrm{UL}}$. This upper limit for the confinement ration is computed from $2.5\,\big(\,\zeta(\mathrm{CR}^{\mathrm{UL}}) - \frac{1+2\alpha+\gamma}{1-\alpha}\,\mathrm{CR}^{\mathrm{UL}}\,\big) = 1$. Notice that for $\sigma_{\mathrm{b}_0}/\sigma_{\mathrm{c}_0} = 1.15$, when $K_{\mathrm{c}} \leq 0.740221743$ then $\mathrm{CR}^{\mathrm{UL}} \leq 1$ and when $K_{\mathrm{c}} \to 0.802325581$, then $\mathrm{CR}^{\mathrm{UL}} \to \infty$. Hence, for this particular choice of equibiaxial to uniaxial compression ratio one may restrict the values of K_{c} to the interval $[0.74, 1.0]$. In addition, for $K_{\mathrm{c}} \in [0.80, 1.0]$, any confinement ratio yields well defined material parameters $a_{\mathrm{c}}(\mathrm{CR})$ and $b_{\mathrm{c}}(\mathrm{CR})$. Figure 2 shows the stress-strain plot in confined uniaxial stress state for C30/37 concrete for various values of K_{c} parameter.

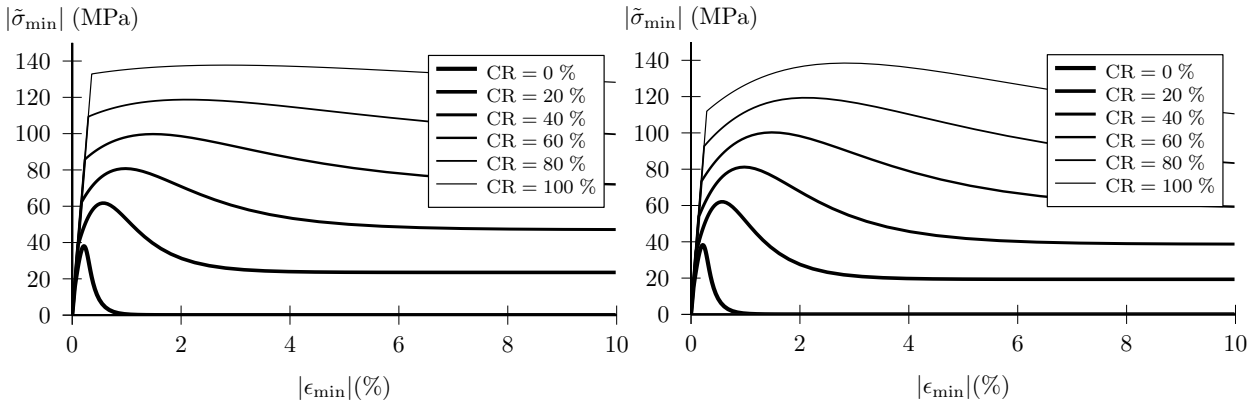

(a) $K_{\mathrm{c}} = 75\%$ (b) $K_{\mathrm{c}} = 80\%$

Figure 2: Total axial stress evolution for various confinement stress levels (C30/37 concrete)

Application to the three dimensional pure shear state

The pure shear state is an example of irrotational strain in which body is elongated in one direction while being shortened perpendicularly in such a way that the total volumetric strain vanishes. Consider a displacement driven pure shear state in three dimensions given by:

$$\boldsymbol{\epsilon} = \mathrm{diag}\big(\,\epsilon\,,\ -\tfrac{1}{2}\,\epsilon\,,\ -\tfrac{1}{2}\,\epsilon\,\big)\ . \tag{58}$$

One can see, that by rotating the principal strain coordinate system in such a way that the first direction becomes collinear with the space diagonal of a cube, i.e. by applying a rotation $\boldsymbol{Q}$ which successively applies the rotation of $\pi/4$ around the third axis and then the rotation of $\mathrm{atan}(1/\sqrt{2})$ around the second axis. The application of such a rotation yields:

$$\boldsymbol{Q}^{\intercal}\cdot\boldsymbol{\epsilon}\cdot\boldsymbol{Q}=\tfrac{1}{2}\begin{pmatrix}0&1&1\\1&0&1\\1&1&0\end{pmatrix}\epsilon\ ,\qquad \boldsymbol{Q}=\tfrac{1}{\sqrt{6}}\begin{pmatrix}\sqrt{2}&\sqrt{2}&\sqrt{2}\\-\sqrt{3}&\sqrt{2}&0\\-1&-1&2\end{pmatrix}\ . \tag{59}$$

It shows that the strain state defined by $\boldsymbol{\epsilon}$ in (58) is equivalent to a shear state with all three shear components equal and normal components zero. From Equation (58), one can also easily infer that the total volumetric strain is nil. At first yield, the elastic strain tensor is diagonal, which together with an isotropic linear elastic material law implies that the stress tensor is diagonal at first yield. Since the deviatoric stress tensor is, as well, diagonal, it implies that the plastic strain rate tensor is diagonal, by virtue of the flow rule and Equation (14). Hence, one can infer that the stress tensor rate is diagonal, which, by recurrence implies that the stress tensor is always diagonal when the strain state is driven by Equation (58). Hence one may write $\tilde{\boldsymbol{\sigma}}=\mathrm{diag}(\,\tilde{\sigma}_1\,,\,\tilde{\sigma}_2\,,\,\tilde{\sigma}_3\,)$. From symmetry considerations we infer that $\tilde{\sigma}_2=\tilde{\sigma}_3$. By definition $\tilde{\sigma}_1=\tilde{\sigma}_{\max}$ is larger than $\tilde{\sigma}_2=\tilde{\sigma}_3=\tilde{\sigma}_{\min}$. Therefore we may write the following expressions for the hydrostatic pressure, $\tilde{p}=(\tilde{\sigma}_{\max}+2\,\tilde{\sigma}_{\min})/3$, and the Mises stress, $\tilde{q}=|\tilde{\sigma}_{\max}-\tilde{\sigma}_{\min}|=\tilde{\sigma}_{\max}-\tilde{\sigma}_{\min}$. Hence, we may write the effective stress tensor in terms of the hydrostatic pressure and the von Mises stress:

$$\tilde{\boldsymbol{\sigma}}=\mathrm{diag}\big(\,\tilde{p}+\tfrac{2}{3}\,\tilde{q}\,,\,\tilde{p}-\tfrac{1}{3}\,\tilde{q}\,,\,\tilde{p}-\tfrac{1}{3}\,\tilde{q}\,\big)\ . \tag{60}$$

Other parameters can be found from Table 5. Notice that $\boldsymbol{T}:\dot{\boldsymbol{\epsilon}}=\dot{\epsilon}$, $\boldsymbol{I}:\dot{\boldsymbol{\epsilon}}=0$, and $\boldsymbol{w}_{\max}\cdot\dot{\boldsymbol{\epsilon}}\cdot\boldsymbol{w}_{\max}=\dot{\epsilon}$.

Table 5: Parameter values in pure shear stress state

Symbol		Value	Symbol		Value	Symbol		Value
$\tilde{p}$	=	$\frac{1}{3}\tilde{\sigma}_{\max}+\frac{2}{3}\tilde{\sigma}_{\min}$	$\Delta T_{\max}$	=	$\frac{2}{3}$	$\boldsymbol{S}$	=	$\mathrm{diag}(\frac{2}{3},-\frac{1}{3},-\frac{1}{3})$
$\tilde{q}$	=	$\tilde{\sigma}_{\max}-\tilde{\sigma}_{\min}$	$\Delta T_{\min}$	=	$-\frac{1}{3}$	3χ	=	$\beta\mathrm{H}(\tilde{\sigma}_{\max})+\gamma\mathrm{H}(-\tilde{\sigma}_{\max})$
T_{av}	=	$\tilde{p}/\tilde{q}$	r	=	$\frac{\langle\tilde{\sigma}_{\max}\rangle+2\langle\tilde{\sigma}_{\min}\rangle}{\lvert\tilde{\sigma}_{\max}\rvert+2\lvert\tilde{\sigma}_{\min}\rvert}$	k_{c}	=	$(1-r)\,n_{\mathrm{c}}\,\frac{\tilde{\sigma}'_{\mathrm{c}}}{G}$
$T_{\max}$	=	$T_{\mathrm{av}}+\frac{2}{3}$	n_{c}	=	$-1+\frac{\langle\tilde{\sigma}_{\max}\rangle}{\tilde{\sigma}_{\mathrm{t}}}$	k_{t}	=	$-r\,n_{\mathrm{t}}\,\frac{\tilde{\sigma}'_{\mathrm{t}}}{G}$
$T_{\min}$	=	$T_{\mathrm{av}}-\frac{1}{3}$	n_{t}	=	$-\frac{\tilde{\sigma}_{\mathrm{c}}}{\tilde{\sigma}_{\mathrm{t}}}\,\frac{\langle\tilde{\sigma}_{\max}\rangle}{\tilde{\sigma}_{\mathrm{t}}}$	$\boldsymbol{w}_{\max}$	=	$(1,0,0)$

Expression of the plastic increment

Substitution of the values exposed in the previous paragraph in Equation (37) gives the expression of $\frac{\dot{\lambda}}{1-d}\frac{\tan\phi}{c(\phi)}=\boldsymbol{\Omega}:\dot{\boldsymbol{\epsilon}}$, whence the plastic increment can be inferred:

$$\boldsymbol{\Omega}:\dot{\boldsymbol{\epsilon}}=\frac{(1+2\,\chi)\,\dot{\epsilon}}{1+2\,\chi+\frac{1-\alpha}{6}\,(2\,k_{\mathrm{t}}-k_{\mathrm{c}})+\big(\,(\alpha+\chi)k+\frac{1-\alpha}{9}\,(k_{\mathrm{c}}+k_{\mathrm{t}})\,\big)c(\phi)}\ . \tag{61}$$

Simplification of Equation (61) leads to

$$\boldsymbol{\Omega}:\dot{\boldsymbol{\epsilon}}=\frac{\dot{\epsilon}}{1+a(\boldsymbol{x})+b(\boldsymbol{x})\,c(\phi)}\ , \tag{62}$$

where a and b can be considered as functions of the hardening flux variables $\epsilon_{\mathrm{c}}^{\mathrm{p}}$ and $\epsilon_{\mathrm{t}}^{\mathrm{p}}$ as well as the current effective stress state, given by $\tilde{p}$ and $\tilde{q}$. Hence, by setting the vector of unknown quantities $\boldsymbol{x} = \{\, \epsilon_{\mathrm{c}}^{\mathrm{p}}\,,\, \epsilon_{\mathrm{t}}^{\mathrm{p}}\,,\, \tilde{p}\,,\, \tilde{q}\,\}$ we may define the functions a and b as follows:

$$a(\boldsymbol{x}) = \frac{\frac{1-\alpha}{6}\,\big(\,2\,k_{\mathrm{t}}(\boldsymbol{x}) - k_{\mathrm{c}}(\boldsymbol{x})\,\big)}{1 + 2\,\chi(\boldsymbol{x})}\;, \tag{63a}$$

$$b(\boldsymbol{x}) = \frac{\big(\,\alpha + \chi(\boldsymbol{x})\,\big)k + \frac{1-\alpha}{9}\,\big(\,k_{\mathrm{c}}(\boldsymbol{x}) + k_{\mathrm{t}}(\boldsymbol{x})\,\big)}{1 + 2\,\chi(\boldsymbol{x})}\;, \tag{63b}$$

where $3\,\chi(\boldsymbol{x}) = \beta(\,\tilde{\sigma}_{\mathrm{c}}(\boldsymbol{x}), \tilde{\sigma}_{\mathrm{t}}(\boldsymbol{x})\,)\,\mathrm{H}(\,\tilde{\sigma}_{\mathrm{max}}(\boldsymbol{x})\,) + \gamma\;\mathrm{H}(\,-\tilde{\sigma}_{\mathrm{max}}(\boldsymbol{x})\,)$. Notice that $\tilde{\sigma}_{\mathrm{c}}(\boldsymbol{x})$ is actually only a function of $\epsilon_{\mathrm{c}}^{\mathrm{p}}$, whereas $\tilde{\sigma}_{\mathrm{t}}(\boldsymbol{x})$ is only a function of $\epsilon_{\mathrm{t}}^{\mathrm{p}}$. The auxiliary quantities k_{c} and k_{t} are also functions of the hardening flux variables and the current stress state:

$$k_{\mathrm{c}}(\boldsymbol{x}) = -\big(\,1 - r(\boldsymbol{x})\,\big)\,\frac{\tilde{\sigma}_{\mathrm{c}}'(\boldsymbol{x})}{G}\,\left(1 - \frac{\langle\tilde{\sigma}_{\mathrm{max}}(\boldsymbol{x})\rangle}{\tilde{\sigma}_{\mathrm{t}}(\boldsymbol{x})}\right)\;, \tag{64a}$$

$$k_{\mathrm{t}}(\boldsymbol{x}) = r(\boldsymbol{x})\,\frac{\tilde{\sigma}_{\mathrm{t}}'(\boldsymbol{x})}{G}\,\left(\frac{\tilde{\sigma}_{\mathrm{c}}(\boldsymbol{x})}{\tilde{\sigma}_{\mathrm{t}}(\boldsymbol{x})}\,\frac{\langle\tilde{\sigma}_{\mathrm{max}}(\boldsymbol{x})\rangle}{\tilde{\sigma}_{\mathrm{t}}(\boldsymbol{x})}\right)\;. \tag{64b}$$

Expression of the plastic strain rates

Recalling that $\tilde{\boldsymbol{s}} = \mathrm{diag}(\,2\,,\,-1\,,\,-1\,)\,\tilde{q}/3$, one can substitute that expression in the flow rule $\dot{\boldsymbol{\epsilon}}^{\mathrm{p}} = \dot{\lambda}/(1-d)\,\boldsymbol{n}_g$, knowing the expression for $\boldsymbol{n}_g$ from Equation (15).

$$\dot{\boldsymbol{\epsilon}}^{\mathrm{p}} = \boldsymbol{\Omega} : \dot{\boldsymbol{\epsilon}}\,\left(\,\mathrm{diag}\big(\,1\,,\,-\tfrac{1}{2}\,,\,-\tfrac{1}{2}\,\big) + \tfrac{1}{3}\,c(\phi)\,\right)\;. \tag{65}$$

Hence one can express the principal plastic strain rates as follows:

$$\dot{\epsilon}_{\mathrm{max}}^{\mathrm{p}} = \frac{\big(\,1 + \frac{1}{3}\,c(\phi)\,\big)\,\dot{\epsilon}}{1 + a(\boldsymbol{x}) + b(\boldsymbol{x})\,c(\phi)}\;, \qquad \dot{\epsilon}_{\mathrm{min}}^{\mathrm{p}} = \frac{\big(\,-\frac{1}{2} + \frac{1}{3}\,c(\phi)\,\big)\,\dot{\epsilon}}{1 + a(\boldsymbol{x}) + b(\boldsymbol{x})\,c(\phi)}\;. \tag{66}$$

The equivalent plastic strains in compression and in tension can be numerically integrated from their rates, $\dot{\epsilon}_{\mathrm{c}}^{\mathrm{p}} = -(1-r)\,\dot{\epsilon}_{\mathrm{min}}^{\mathrm{p}}$ and $\dot{\epsilon}_{\mathrm{t}}^{\mathrm{p}} = r\,\dot{\epsilon}_{\mathrm{max}}^{\mathrm{p}}$, respectively. Hence we have:

$$\dot{\epsilon}_{\mathrm{c}}^{\mathrm{p}} = \frac{\big(\,1 - r(\boldsymbol{x})\,\big)\,\big(\,\frac{1}{2} - \frac{1}{3}\,c(\phi)\,\big)\,\dot{\epsilon}}{1 + a(\boldsymbol{x}) + b(\boldsymbol{x})\,c(\phi)}\;, \qquad \dot{\epsilon}_{\mathrm{t}}^{\mathrm{p}} = \frac{r(\boldsymbol{x})\,\big(\,1 + \frac{1}{3}\,c(\phi)\,\big)\,\dot{\epsilon}}{1 + a(\boldsymbol{x}) + b(\boldsymbol{x})\,c(\phi)}\;. \tag{67}$$

Expression of the effective stress rate

The elastic stress-strain rate relationship is $\dot{\tilde{\boldsymbol{\sigma}}} = 2\,\mu\,(\dot{\boldsymbol{\epsilon}} - \dot{\boldsymbol{\epsilon}}^{\mathrm{p}}) + \lambda\,\big(\,\mathrm{tr}(\dot{\boldsymbol{\epsilon}}) - \mathrm{tr}(\dot{\boldsymbol{\epsilon}}^{\mathrm{p}})\,\big)\,\boldsymbol{I}$. Substituting the expression of the plastic strain rate as given in Equation (65) leads to:

$$\dot{\tilde{\boldsymbol{\sigma}}} = 2\,\mu\;(\,\dot{\epsilon} - \boldsymbol{\Omega} : \dot{\boldsymbol{\epsilon}}\,)\;\mathrm{diag}\big(\,1\,,\,-\tfrac{1}{2}\,,\,-\tfrac{1}{2}\,\big) - \left(\frac{2\,\mu}{3} + \lambda\right)\,\boldsymbol{\Omega} : \dot{\boldsymbol{\epsilon}}\,c(\phi)\,\boldsymbol{I}\;. \tag{68}$$

Substituting the Lamé parameters by the shear and bulk moduli in Equation (68) as well as substituting the expression of $\boldsymbol{\Omega} : \dot{\boldsymbol{\epsilon}}$ by the one given in Equation (62) leads to the following formulation:

$$\dot{\tilde{\boldsymbol{\sigma}}} = G\,\frac{\big(\,a(\boldsymbol{x}) + b(\boldsymbol{x})\,c(\phi)\,\big)\,\dot{\epsilon}}{1 + a(\boldsymbol{x}) + b(\boldsymbol{x})\,c(\phi)}\,\mathrm{diag}\big(\,2\,,\,-1\,,\,-1\,\big) - K\,\frac{c(\phi)\,\dot{\epsilon}}{1 + a(\boldsymbol{x}) + b(\boldsymbol{x})\,c(\phi)}\,\boldsymbol{I}\;. \tag{69}$$

Hence the maximum and minimum principal effective stress rates are given as follows:

$$\dot{\tilde{\sigma}}_{\max} = \frac{2\,G\,\big(\,a(\boldsymbol{x}) + b(\boldsymbol{x})\,c(\phi)\,\big) - K\,c(\phi)}{1 + a(\boldsymbol{x}) + b(\boldsymbol{x})\,c(\phi)}\,\dot{\epsilon}\;, \tag{70a}$$

$$\dot{\tilde{\sigma}}_{\min} = -\frac{G\,\big(\,a(\boldsymbol{x}) + b(\boldsymbol{x})\,c(\phi)\,\big) + K\,c(\phi)}{1 + a(\boldsymbol{x}) + b(\boldsymbol{x})\,c(\phi)}\,\dot{\epsilon}\;. \tag{70b}$$

Further recalling that $\dot{\tilde{p}} = (\dot{\tilde{\sigma}}_{\max} + 2\,\dot{\tilde{\sigma}}_{\min})/3$ and that $\dot{\tilde{q}} = \dot{\tilde{\sigma}}_{\max} - \dot{\tilde{\sigma}}_{\min}$. Hence using equations (70a) and (70b) one ends up with the following expressions for the effective hydrostatic pressure rate and the effective Mises equivalent stress rate:

$$\dot{\tilde{p}} = -K\,\frac{c(\phi)}{1 + a(\boldsymbol{x}) + b(\boldsymbol{x})\,c(\phi)}\,\dot{\epsilon}\;, \qquad \dot{\tilde{q}} = 3\,G\,\frac{\big(\,a(\boldsymbol{x}) + b(\boldsymbol{x})\,c(\phi)\,\big)}{1 + a(\boldsymbol{x}) + b(\boldsymbol{x})\,c(\phi)}\,\dot{\epsilon}\;. \tag{71}$$

Expression of the numerical ODE to solve

Stacking equations (67) and (71) leads to a first order ODE $\dot{\boldsymbol{x}} = \boldsymbol{F}(\boldsymbol{x})\,\dot{\epsilon}$, where the components of the right hand side vector valued function $\boldsymbol{F}$ are given as follows:

$$F_1(\boldsymbol{x}) = \frac{\big(1 - r(\boldsymbol{x})\big)\,\big(\,\frac{1}{2} - \frac{1}{3}\,c(\phi)\,\big)}{1 + a(\boldsymbol{x}) + b(\boldsymbol{x})\,c(\phi)}\;, \qquad F_3(\boldsymbol{x}) = -K\,\frac{c(\phi)}{1 + a(\boldsymbol{x}) + b(\boldsymbol{x})\,c(\phi)}\;, \tag{72a}$$

$$F_2(\boldsymbol{x}) = \frac{r(\boldsymbol{x})\,\big(1 + \frac{1}{3}\,c(\phi)\,\big)}{1 + a(\boldsymbol{x}) + b(\boldsymbol{x})\,c(\phi)}\;, \qquad F_4(\boldsymbol{x}) = 3\,G\,\frac{\big(\,a(\boldsymbol{x}) + b(\boldsymbol{x})\,c(\phi)\,\big)}{1 + a(\boldsymbol{x}) + b(\boldsymbol{x})\,c(\phi)}\;. \tag{72b}$$

The easiest way to solve the ODE $\dot{\boldsymbol{x}} = \boldsymbol{F}(\boldsymbol{x})\,\dot{\epsilon}$ subject to the yield condition $f(\boldsymbol{x}) \leq 0$ is to use constant time increment forward Euler time integration to get the predictor $\hat{\boldsymbol{x}}^{(i+1)} = \boldsymbol{x}^{(i)} + \boldsymbol{F}(\boldsymbol{x}^{(i)})\,\dot{\epsilon}\,\Delta t$. One can then assume that the corrected internal hardening variables are the predicted ones: $\{\,(\epsilon_{\mathrm{c}}^{\mathrm{p}})^{(i+1)}\,,\,(\epsilon_{\mathrm{t}}^{\mathrm{p}})^{(i+1)}\,\} = \{\,(\hat{\epsilon}_{\mathrm{c}}^{\mathrm{p}})^{(i+1)}\,,\,(\hat{\epsilon}_{\mathrm{t}}^{\mathrm{p}})^{(i+1)}\,\}$. The stress variables, however have to be corrected so that the yield condition is satisfied. One can either implement an orthogonal projection or a projection along the vector. The latter is implemented in this case choosing the corrected values $\{\,\tilde{p}^{(i+1)}\,,\,\tilde{q}^{(i+1)}\,\}$ to be proportional to the predicted values, $\{\,\hat{\tilde{p}}^{(i+1)}\,,\,\hat{\tilde{q}}^{(i+1)}\,\}$ such that $f(\,(\epsilon_{\mathrm{c}}^{\mathrm{p}})^{(i+1)}\,,\,(\epsilon_{\mathrm{t}}^{\mathrm{p}})^{(i+1)}\,,\,\xi\,\hat{\tilde{p}}^{(i+1)}\,,\,\xi\,\hat{\tilde{q}}^{(i+1)}\,) = 0$, where $\xi > 0$ is the factor of proportionality to be found. The proposed time integration scheme worked out well for all the example cases that were computed.

Discussion

Analysis of the results of the CDP material model response to monotonic displacement-driven loading in each of the previously defined simple stress states helps in obtaining a clearer insight of the overall behavior of the model. The discussion focuses on general comments on internal hardening variable evolution in pure shear, stress-strain evolution in pure shear, element size dependency, the effect of volumetric dilation in pure shear and comments on element deletion algorithms.

Internal hardening variable evolution in pure shear

Numerical solutions of the ODE $\dot{\boldsymbol{x}} = \boldsymbol{F}(\boldsymbol{x})\,\dot{\epsilon}$, describing the pure shear state, can be plotted for various values of constant loading rates, $\dot{\epsilon}$. Each plot is given for three values of the dilation angle, low, moderate and high. The hardening variables $\epsilon_{\mathrm{t}}^{\mathrm{p}}$ and $\epsilon_{\mathrm{c}}^{\mathrm{p}}$, are plotted

as evolutions in terms of the maximum principal total strain in Figures 4 and 5. Notice a reduced increase of the internal hardening variables as the dilation angle increases, which can be interpreted as a reduction in plastic processes and increase in elastic processes for high values of dilation angle. Also notice that in contrary to the internal hardening variable in compression, the internal hardening variable in tension quickly reaches its asymptotic value. The implication of this fact is that for low deformations, pure shear response is driven by the tensile behavior, but for large deformations the same pure shear response is driven by the compressive behavior. Whether this kind of response is physically relevant is subject to debate.

Stress-strain evolution in pure shear

From the primary variables of the ODE, $\boldsymbol{x}$, one can derive other quantities of interest. Figures 6 and 7 show the maximum principal effective stress and the minimum principal effective stress evolution with respect to the maximum and minimum principal total strains, respectively. Notice here a major dependence of the maximum principal effective stress evolution on the dilation angle and minor dependence on the K_c ratio. Likewise, notice a moderate dependence of the minimum principal effective stress evolution on the dilation angle. The maximum principal stress shows strong strain softening behavior after the pure shear maximum stress is reached. In contrary to the uniaxial tensile response, which asymptotically decreases to zero, the pure shear response shows almost linear decrease of maximum stress with a sign change for a finite value of the maximum principal total strain. In other words, the computational response of the CDP model in pure shear shows more brittle behavior than the uniaxial tensile response. Again, whether this kind of response is physically correct is subject to debate.

Element size dependency in pure shear

Another issue that should be noticed when comparing uniaxial tensile and pure shear responses is element size dependence. Notice, that as shown in the stress-strain response in uniaxial tension, Figure 1a, the Hillerborg regularization, [16, 17, 18], results in a unique value for the tensile fracture energy independently of the element size. However, looking at Figure 6, one can clearly see that the pure shear fracture energy of the 100mm element is tenfold compared to the pure shear fracture energy of the 10mm element.

Effect of the volumetric dilation

Looking at the maximum principal effective stress plot, Figure 6, one can observe a softening behavior up to a point when the maximum principal effective stress becomes negative, which means that one has compressive stresses in all principal directions even though the maximum principal strain is tensile. The explanation to this unphysical behavior is that the part of volumetric dilation in pure shear becomes unrealistically large. Therefore, the natural interpretation of this numerical behavior would be to consider a shear failure in the given material point. Figure 3 shows the value of this *cutoff shear strain* value as a function of the angle of dilation. Notice, that the strain rate as well as the element characteristic length almost do not influence the value of the cutoff shear strain. This is the reason why the fittings have been done using the quasi-static rate only.

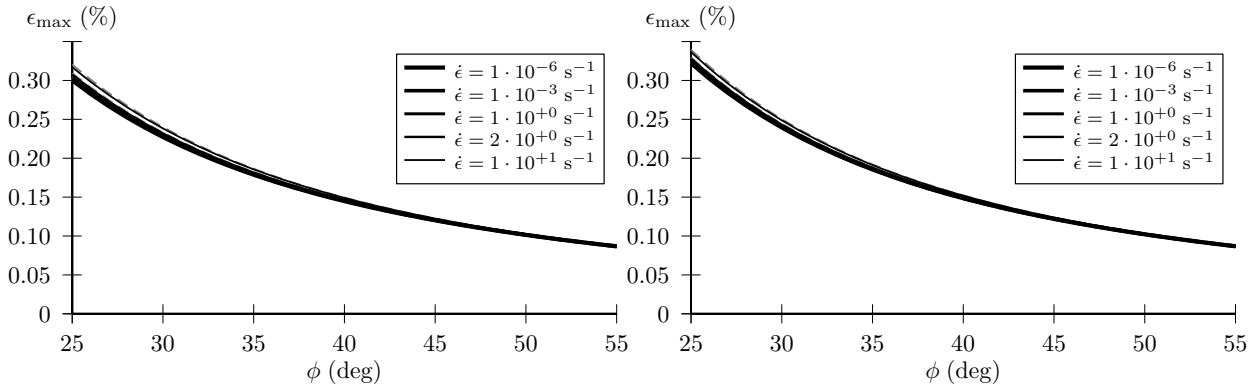

(a) $K_c = 0.75$ (b) $K_c = 0.80$

Figure 3: Cutoff shear strain as function of the angle of dilation (C30/37 concrete, solid: l_{ch}=100mm, dashed: l_{ch}=10mm)

Comments on element deletion algorithms

In finite element simulations, fragmentation of the concrete body is materialized by changing the element mesh topology, in other words by removing elements during the simulation in appropriate situations. This element removal algorithm has traditionally been based on the evolution of internal hardening variable in compression, [12, 9, 10]. It has been shown in Figure 4 that the evolution of the internal hardening variable in tension quickly plateaus to an asymptotic value. On contrary, Figure 5 shows that the evolution of the internal variable in compression is almost linear, making it a suitable candidate for element removal control.

However, other candidate variables need also to be investigated. In particular, a candidate for the element deletion criterion in pure shear failure is discussed here. It has been shown above that in a pure shear stress state one can define a shear strain cutoff value as per Figure 3. In many applications the fragmentation of concrete occurs shear bands. This is the case especially in hard missile impact simulations, where the shear band is formed on the boundary of the shear cone. It is assumed that in a concrete shear band the strain state is close to the pure shear strain state. Hence, one can consider, for instance, the octahedral strain as measure of the pure shear content of the actual strain state. Although detailed description of such a shear based element deletion criterion is out of scope of this research, one can propose the following broad guideline. By using the condition where the current pure shear strain at a material point is less than the cutoff shear strain, which is a material property, one can switch on the shear failure flag. Then, as long as the failed element is still properly confined by neighboring elements it is not yet removed from the computation. Only when confinement drops below a critical level, the element that has previously failed in shear is ready to be removed.

Summary

This paper is a tentative to open the "black box" of the CDP model as implemented in Abaqus. First, a general expression of the plastic increment has been provided in Equation (37). This expression has then been applied to three stress states: the uniaxial tensile stress state, the confined uniaxial compressive stress state and the pure shear stress state. In simulations where modeling the fragmentation of concrete is necessary,

element removal criteria need to be implemented in order to materialize macroscopic crack formation. By investigating these simple stress states one gets clues about how the implementation of the element deletion criteria needs to be done. As an example, one can mention the simulation of impact loaded concrete structures because they characterize different phenomena, namely spalling and scabbing, formation of the confined plug and formation of the shear cone, respectively. Since the formation of the shear cone has to be materialized in impact simulations by removal of elements located in the shear band, it is natural to select an element removal criterion based on the CDP material model behavior in pure shear. Further investigations are necessary to test the validity of this hypothesis.

References

[1] Simulia. *Abaqus 6.14-5 Manual*. Dassault Simulia, 2016.

[2] J. Lubliner, J. Oliver, S Oller, and E. Oñate. A plastic-damage model for concrete. *Int.J. of Solids and Structure*, 25(3):299–326, 1989. doi:10.1016/0020-7683(89)90050-4

[3] J.H. Lee. *Theory and implementation of plastic-damage model for concrete structures under cyclic and dynamic loading*. PhD dissertation, University of Berkley, California, 1996.

[4] J.H. Lee and G. Fenves. Plastic-damage model for cyclic loading of concrete structures. *Journal of Engineering mechanics*, 124(8):892–900, 1998. doi:10.1061/(ASCE)0733-9399(1998)124:8(892)

[5] T. Gabet. *Thèse: Comportement triaxial du béton sous fortes contraintes: influence du trajet de chargement*. Université Joseph Fourier, Grenoble, 2006.

[6] X.D. Vu. *Vulnérabilité des ouvrages en béton sous impact : Caractérisation, modélisation, et validation*. Université Joseph Fourier, Grenoble, 2013.

[7] CEN European Committee for Standardization. *Eurocode 2 - Design of concrete structures*. Finnish Standards Association SFS, 1992.

[8] J.R. Klepaczko and A. Brara. An experimental method for dynamic tensile testing of concrete spalling. *International Journal of Impact Engineering*, 2001. doi:10.1016/S0734-743X(00)00050-6

[9] J Rodriguez, F. Martinez, and J. Marti. Concrete constitutive model, calibration and applications. *2013 SIMULIA Community Conference*, 2013.

[10] A. Fedoroff, J. Kuutti, and A. Saarenheimo. A physically motivated element deletion criterion for the concrete damage plasticity model. In *SMiRT-24 transactions*. International Association for Structural Mechanics in Reactor Technology, 2017.

[11] A. Fedoroff. Continuum damage plasticity for concrete modeling. *VTT reports, VTT-R-00331-17*, 2017.

[12] L. Agardh and L. Laine. 3d fe-simulation of high-velocity fragment perforation of reinforced concrete slabs. *International Journal of Impact Engineering, 911-922*, 1999. doi:10.1016/S0734-743X(99)00008-1

[13] J. Eibl and H. Bachmann. Festigkeisverhalten von beton unter dem einfluenss der dehngeschwindigkeit. *Massivbau Baustofftechnologie Karlsruhe*, 1993.

[14] J. Weerheijm and I. Vegt. How to Determine the Dynamic Fracture Energy of Concrete. Theoretical Considerations and Experimental Evidence. *Applied Mechanics and Materials, 51-56*, 2011. doi:10.4028/www.scientific.net/AMM.82.51

[15] F. Min, Z. Yao, and T. Jiang. Experimental and numerical study on tensile strength of concrete under different strain rates. *The Scientific World Journal*, 2014. doi:10.1155/2014/173531

[16] A. Hillerborg. The theoretical basis of a method to determine the fracture energy gf of concrete. *Materials and structures*, pages 291–296, 1985. doi:10.1007/BF02472919

[17] A. Hillerborg, M. Modéer, and P. Pettersson. Analysis of crack formation and and crack growth in concrete by means of fracture mechanics and finite elements. *Cement Concrete Research*, 6:773–782, 1976. doi:10.1016/0008-8846(76)90007-7

[18] A. Hillerborg. A model for fracture analysis. *Lund institute of technology report TVBM-3005*, 1978.

Alexis Fedoroff, Kim Calonius and Juha Kuutti
VTT Technical Research Centre of Finland
Kemistintie 3, Espoo, P.O. Box 1000, FI-02044 VTT, Finland
`Alexis.Fedoroff@vtt.fi, Kim.Calonius@vtt.fi, Juha.Kuutti@vtt.fi`

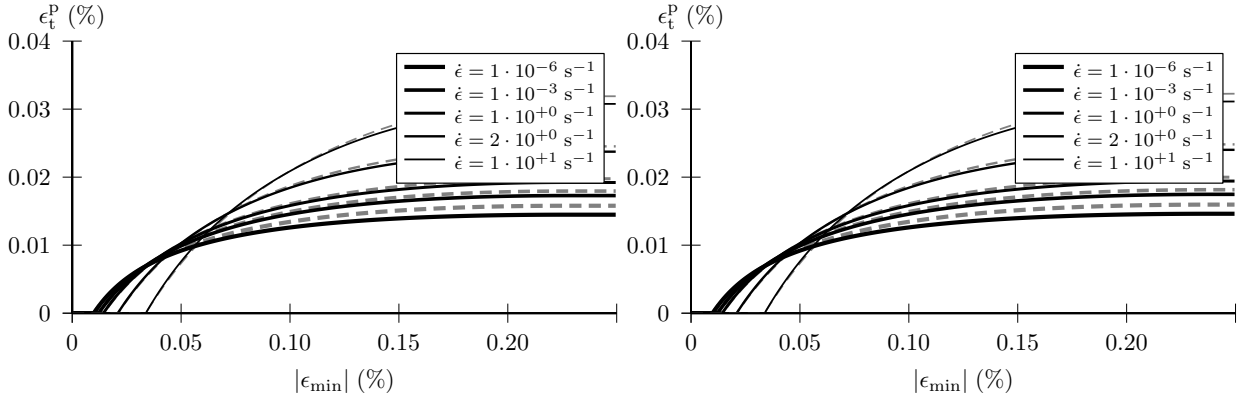

(a) $\phi = 30\,\text{deg}$, $K_c = 0.75$

(b) $\phi = 30\,\text{deg}$, $K_c = 0.80$

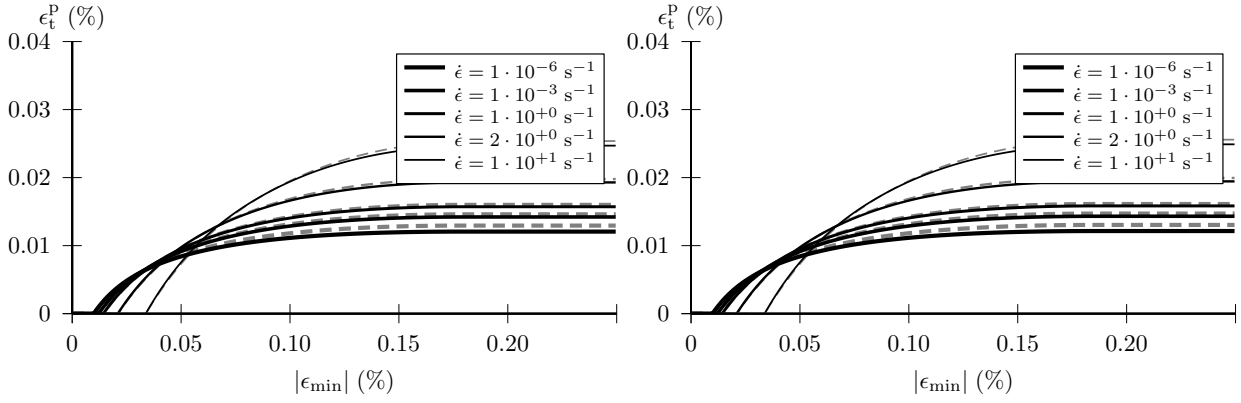

(c) $\phi = 35\,\text{deg}$, $K_c = 0.75$

(d) $\phi = 35\,\text{deg}$, $K_c = 0.80$

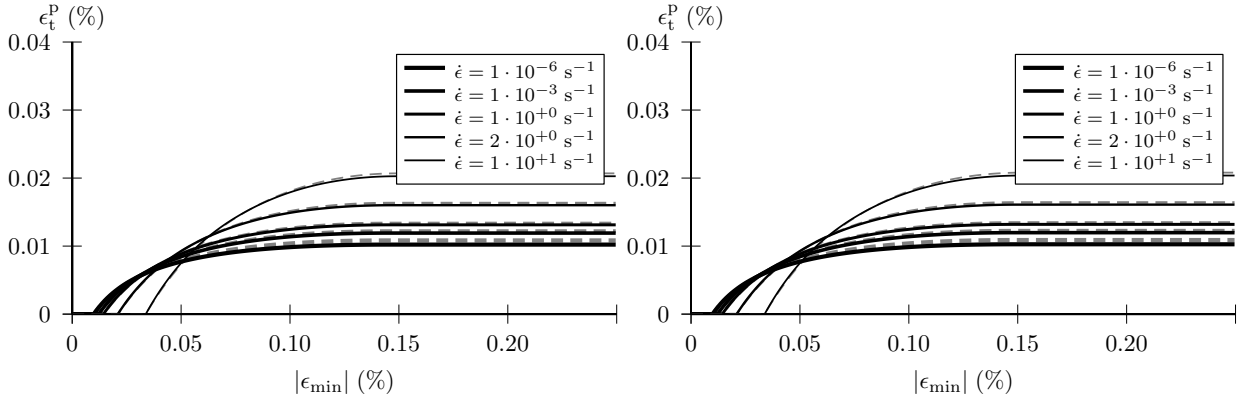

(e) $\phi = 40\,\text{deg}$, $K_c = 0.75$

(f) $\phi = 40\,\text{deg}$, $K_c = 0.80$

Figure 4: Internal tensile hardening variable evolution in pure shear (C30/37 concrete, solid: l_{ch}=100mm, dashed: l_{ch}=10mm)

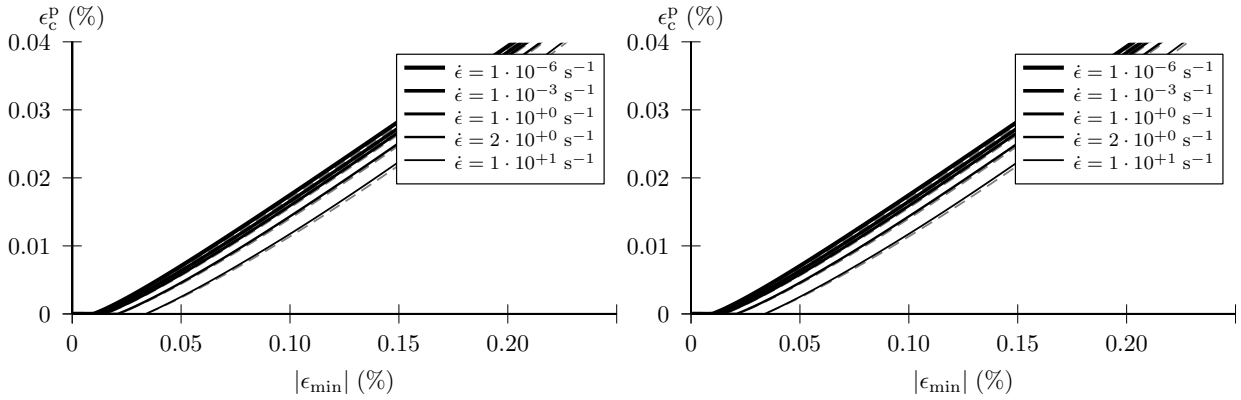

(a) $\phi = 30\,\text{deg}$, $K_c = 0.75$

(b) $\phi = 30\,\text{deg}$, $K_c = 0.80$

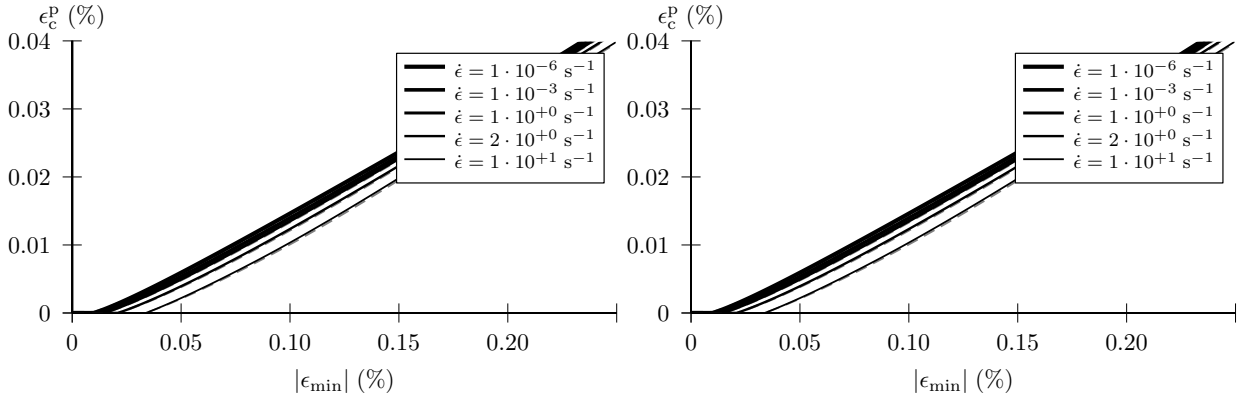

(c) $\phi = 35\,\text{deg}$, $K_c = 0.75$

(d) $\phi = 35\,\text{deg}$, $K_c = 0.80$

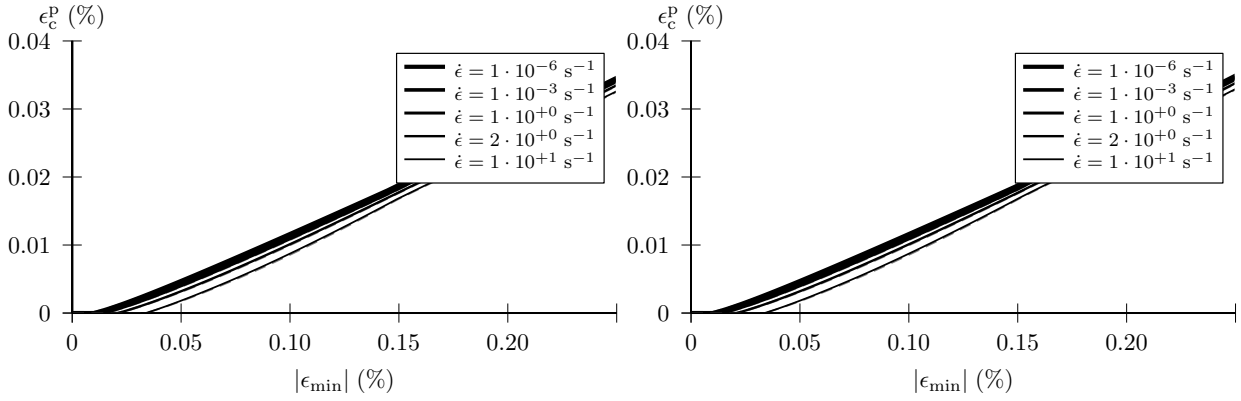

(e) $\phi = 40\,\text{deg}$, $K_c = 0.75$

(f) $\phi = 40\,\text{deg}$, $K_c = 0.80$

Figure 5: Internal compressive hardening variable evolution in pure shear (C30/37 concrete, solid: l_{ch}=100mm, dashed: l_{ch}=10mm)

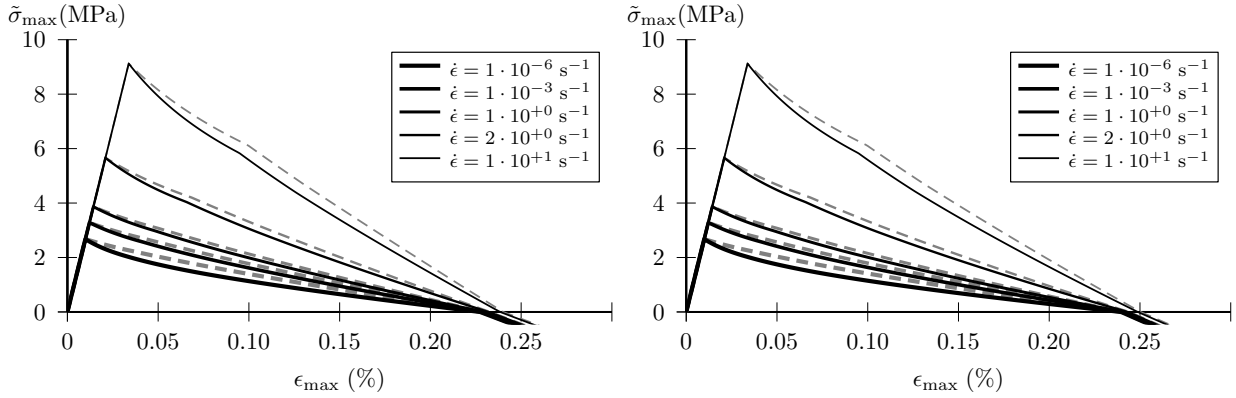

(a) $\phi = 30\,\text{deg}$, $K_\text{c} = 0.75$

(b) $\phi = 30\,\text{deg}$, $K_\text{c} = 0.80$

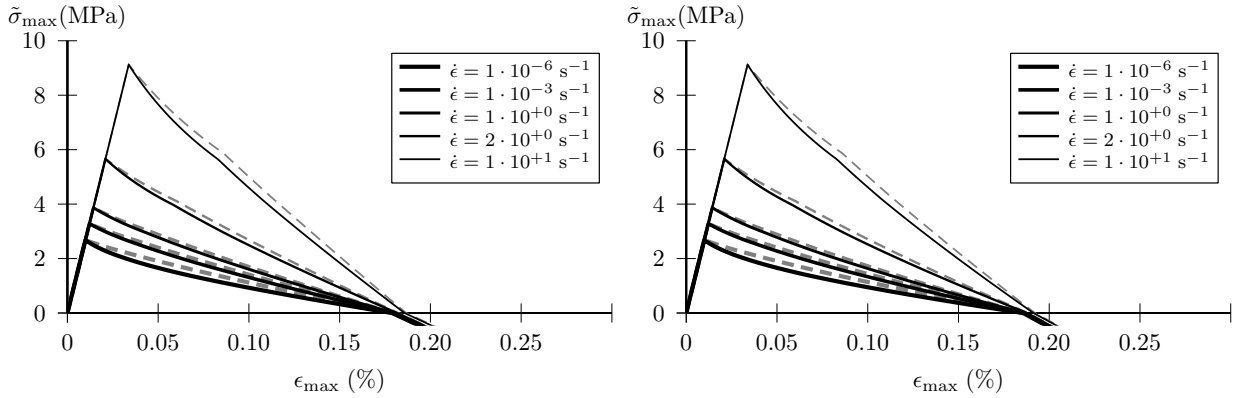

(c) $\phi = 35\,\text{deg}$, $K_\text{c} = 0.75$

(d) $\phi = 35\,\text{deg}$, $K_\text{c} = 0.80$

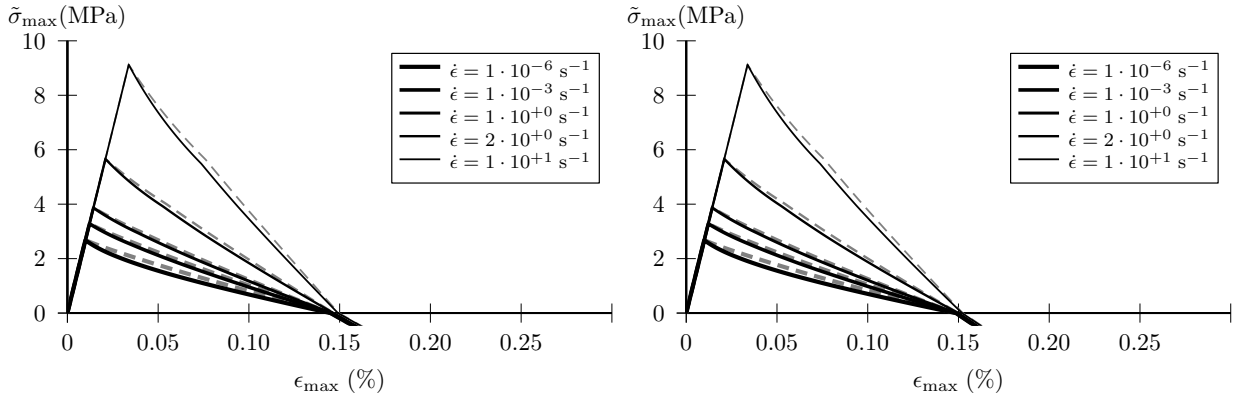

(e) $\phi = 40\,\text{deg}$, $K_\text{c} = 0.75$

(f) $\phi = 40\,\text{deg}$, $K_\text{c} = 0.80$

Figure 6: Maximum principal effective stress evolution in pure shear (C30/37 concrete, solid: l_ch=100mm, dashed: l_ch=10mm)

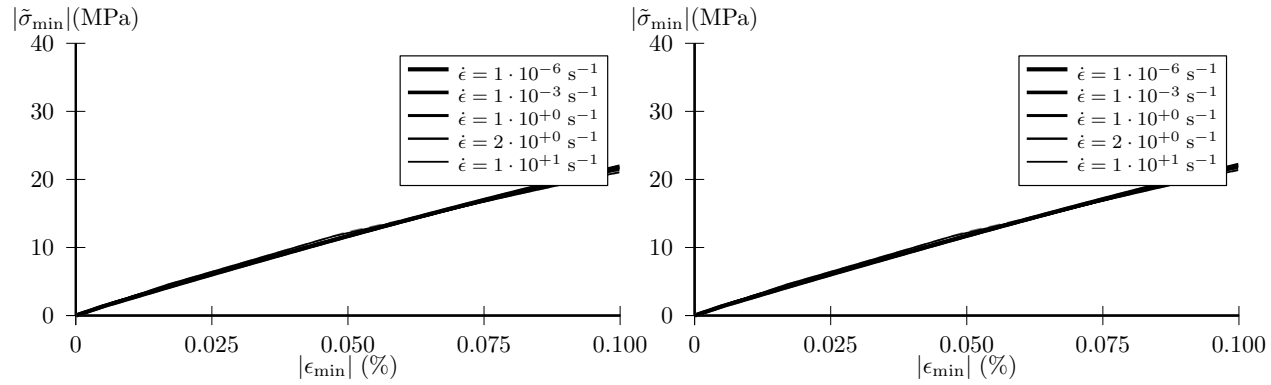

(a) $\phi = 30\,\text{deg}$, $K_\text{c} = 0.75$

(b) $\phi = 30\,\text{deg}$, $K_\text{c} = 0.80$

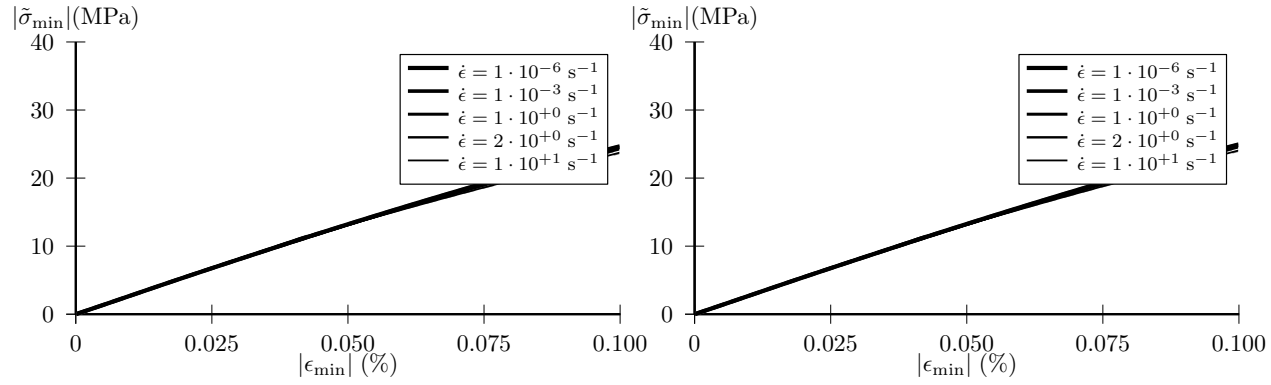

(c) $\phi = 35\,\text{deg}$, $K_\text{c} = 0.75$

(d) $\phi = 35\,\text{deg}$, $K_\text{c} = 0.80$

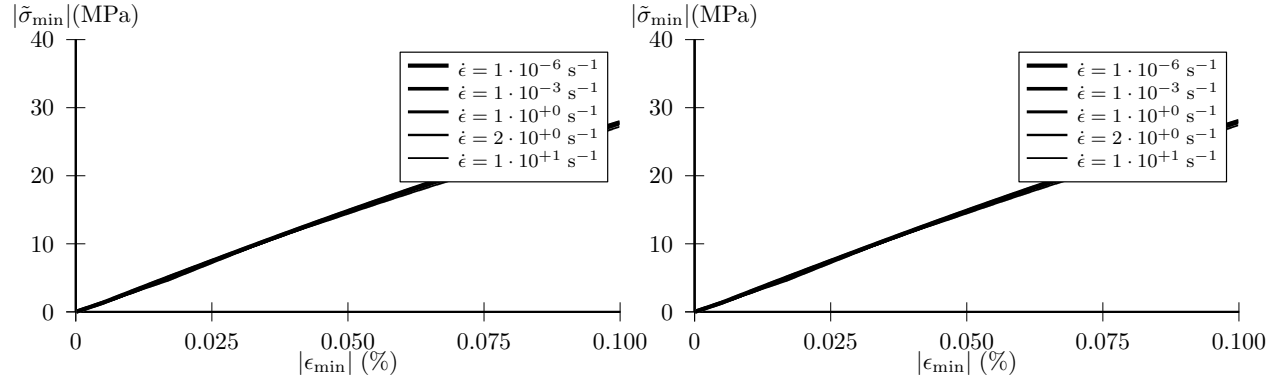

(e) $\phi = 40\,\text{deg}$, $K_\text{c} = 0.75$

(f) $\phi = 40\,\text{deg}$, $K_\text{c} = 0.80$

Figure 7: Minimum principal effective stress evolution in pure shear (C30/37 concrete, solid: l_ch=100mm, dashed: l_ch=10mm)